

A Semi-Infinite Closed-Form Analytical Solution For Solidification Under Convective Boundary Condition

I.L. Ferreira^{*}, G.E.M. Santos Júnior, A.L.S. Moreira

Faculty Of Mechanical Engineering, Federal University Of Pará, UFPA, Augusto Corrêa Avenue 1, 66075-110, Belém, PA, Brazil

**Corresponding Author: ileao@ufpa.br*

Abstract

Solidification and fusion are important processes applied in several fields of science and technology. Recently, FAR beyond the realms of materials science and metallurgy, many applications have risen in latent heat thermal energy storage and melting and growth of ice plates. Due to the relative difficulty in obtaining numerical solutions for moving boundary problems for a wide range of space and time scales. No studies in the literature consider a comprehensive first and second-order treatment of Biot number for phase change. This work proposes four closed-form solutions for the transient solidification of pure and eutectic materials for one- and three-dimensional semi-infinite slabs considering convective boundary conditions and melting superheat. This approach can predict wide space and time scales by adding a first-order term in the parabolic profile to address the transition from second to first-order similarity variables.

Keywords: *Partial differential equation; Convective boundary condition; Unsteady analytical solution; Moving boundary problem; Semi-infinite slab.*

Date of Submission: 27-04-2025

Date of Acceptance: 07-05-2025

I. Introduction

It is well established that solidification and fusion are important processes applied in several fields of science and technology [1]. Recently, for example, far beyond the fields of materials science and metallurgy, many applications have emerged with regard to latent heat thermal energy storage (LHTES) and other methods related to the melting and growth of ice sheets. On the other hand, the properties of materials are strongly dependent on their composition, manufacturing process and particularly their structure. Solidification, for example, plays a fundamental role in obtaining homogeneous materials and in controlling their structure in some industrial processes, such as casting, laser welding, surface remelting and continuous casting. Therefore, the study of the complex relationship between solidification parameters and the resulting microstructure is of growing importance in the field of metallurgy for the development of increasingly suitable methods for quality casting in the shipping, automotive, electronics and aerospace industries since the physical, metallurgical, mechanical, and electrochemical properties of most materials depend mainly on the level of control that can be achieved during liquid-solid phase change. Nevertheless, in many cases, complete details of the physical mechanisms related to the formation of various types of structures in the obtained materials are not yet known [2].

By analysing theoretically and experimentally the solidification process, certain variables that effectively act on the liquid-solid transformation are investigated because, during phase change, various physical-chemical effects occur, which, if not properly controlled, can compromise the performance and quality of the final casting part. In the initial moments when the phenomenon occurs, heat transfer is one of the main factors that has a significant effect on the thermal variables involved, especially the cooling rate (TR) [3,4]. Thus, a better understanding of the effect of thermal parameters on the formation of structural aspects is essential for planning some industrial manufacturing processes.

It is known that heat conduction with phase change due to melting-freezing occurs in the transient regime. The mathematical treatment of solidification becomes more challenging because it results in differential equations with nonlinear boundary conditions at the moving interface [5-7], almost always requiring the establishment of physical or mathematical simplifying hypotheses from real conditions so that analytical solutions may be made viable. Despite this, numerous mathematical approaches have been proposed to provide an adequate theoretical background for modelling the mechanisms by which heat is transferred in both the solid and liquid domains in transformation as well as in the cooling fluid.

Studies have proposed analytical methods and numerical solutions to describe solidification, the results of which, in some cases, are very close to those observed in various cases of practical interest. Nonetheless, it is imperative to emphasize that the precision and control of their respective outcomes are directly correlated with

the properties of interest of the material under investigation, the boundary conditions assumed, and the physical and/or mathematical simplifications accepted. In this sense, the analytical methods [8-19] are limited to the study of solidification in slabs due to the greater simplicity of the mathematical treatment as a result of their geometric characteristics, which is the only case for which an exact solution has been obtained thus far. Therefore, they present considerable limitations from the point of view of their practical application. One of the main advantages of numerical methods [20-34] is that they allow more realistic boundary conditions to be accepted, for which it would not be possible to obtain analytical solutions. The accuracy of these methods is generally quite high, but they require the use of computational resources as well as a certain amount of complexity. These methods generally lead to greater agreement with the results observed in practice. On the other hand, a large number of experimental studies have also been performed to fulfil the same objective [35-54]. Another interesting technique that has been widely used to determine the unsteady thermal variables acting during solid-liquid phase change is the inverse heat conduction problem (IHCP), which is based on a mathematical description of the physical mechanisms of the process supplemented with experimentally obtained temperature measurements in metals and/or molds. The inverse problem is solved by adjusting the parameters in the mathematical description to minimize the difference between the model-computed values and the experimental measurements [55-57].

In this work, closed-form solutions for the transient solidification of both pure and eutectic materials are derived for one- and three-dimensional semi-infinite slabs considering convective boundary conditions and melting superheat.

II. Mathematical Formulation

Analytical solutions are derived for one-phase and two-phase transient solidification of pure and eutectic materials in one- and three-dimensional problems considering anisotropic media. An anisotropic medium can be characterised by a dependency on thermophysical properties and space coordinates, i.e., for density $\rho = \rho(x, y, z) = \sqrt{\rho_x^2 + \rho_y^2 + \rho_z^2}$, specific heat $c_p = c_p(x, y, z) = \sqrt{c_{px}^2 + c_{py}^2 + c_{pz}^2}$, thermal conductivity $k = k(x, y, z) = \sqrt{k_x^2 + k_y^2 + k_z^2}$ and thermal diffusivity, $\alpha = \alpha(x, y, z) = \sqrt{\alpha_x^2 + \alpha_y^2 + \alpha_z^2}$. It is true, as for a 3D problem, solutions are independently obtained in each direction $\theta(x, y, z, t) = \theta_x(x, t) \cdot \theta_y(y, t) \cdot \theta_z(z, t)$ and coupled with the solution of the similarity variable ϕ considering the moving boundary interface, $\rho_S L \frac{ds}{dt} = (k_S \nabla T_S)|_{X=-s} - (k_L \nabla T_L)|_{X=+s}$, and position $s = \sqrt{s_x^2 + s_y^2 + s_z^2}$.

One-dimensional One-Phase Moving Boundary Problem

For the freezing/solidification of a pure metal/compound at the fusion temperature or eutectic temperature, as shown in Figure 1, the governing partial differential equation and the initial and boundary conditions for a semi-infinite slab are given by

$$\frac{\partial^2 T_S}{\partial x^2} = \frac{1}{\alpha_S} \frac{\partial T_S}{\partial t} \quad 0 < x < s(t) \quad (1)$$

$$t = 0, \quad 0 < x < +\infty, \quad T = T_F \quad (2)$$

$$t > 0, x = 0, -k \left. \frac{\partial T}{\partial x} \right|_{x=0} = h(T - T_\infty) \quad (3)$$

$$t > 0, x = s(t), T_S = T_F \quad (4)$$

$$t > 0, x \rightarrow +\infty, T_S = T_F \quad (5)$$

$$\rho_S L \frac{ds}{dt} = k_S \left. \frac{\partial T_S}{\partial x} \right|_{x=-s} \quad (6)$$

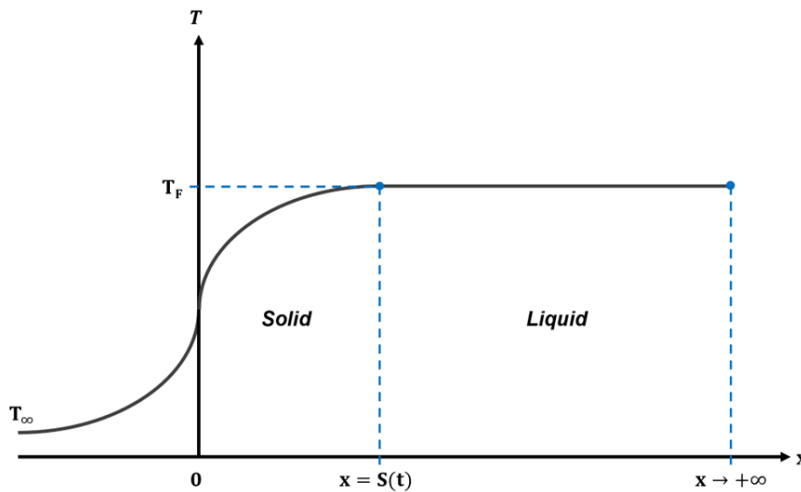


Figure 1 Schematic representation of one-phase transient solidification.

The base solution for the solid phase is a well-known 1D one for a semi-infinite slab whose boundary condition at $z = 0$ is of the third kind [58] for nonreaction problems. The temperature profile dependence on time and space can be expressed as

$$T(x, t) - T_{\infty} = A_S + B_S \left\{ \operatorname{erfc} \left(\frac{x}{2\sqrt{\alpha_S t}} \right) - \exp \left(\frac{h x}{k_S} + \frac{h^2 \alpha_S t}{k_S^2} \right) \operatorname{erfc} \left(\frac{x}{2\sqrt{\alpha_S t}} + \frac{h \sqrt{\alpha_S t}}{k_S} \right) \right\} \quad (7)$$

where A_S and B_S are constants determined from the solid interface at $s(t) = 0$ and $s(t) = s$.

For $s = 0$,

$$T_S(s = 0, t) = T_{\infty} = A_S + B_S \quad (8)$$

which is a consequence of a convective boundary condition already applied in the solution for $x = 0$ when the base function $T(x, t)$ is derived, so that $T_S(s = 0, t)$ cannot be admitted by $T_S(x, t)$. In this sense, B_S is a constant value that can be found as a function of the temperature profile at $x = 0$.

For $x = s$,

$$T_S(x = s, t) = T_F = A_S + B_S \left\{ \operatorname{erfc} \left(\frac{s}{2\sqrt{\alpha_S t}} \right) - \exp \left(\frac{h s}{k_S} + \frac{h^2 \alpha_S t}{k_S^2} \right) \operatorname{erfc} \left(\frac{s}{2\sqrt{\alpha_S t}} + \frac{h \sqrt{\alpha_S t}}{k_S} \right) \right\} \quad (9)$$

By taking the parabolic profile $\frac{s}{2\sqrt{\alpha_S t}}$ and writing it as a similarity variable $\varphi(s, t) = \frac{s}{2\sqrt{\alpha_S t}}$, Eq. (9) becomes

$$T_F = A_S + B_S \left\{ \operatorname{erfc}(\varphi) - \exp \left(\frac{h s}{k_S} + \frac{h^2 s^2}{4\varphi^2 k_S^2} \right) \operatorname{erfc} \left(\varphi + \frac{h s}{2\varphi k_S} \right) \right\} \quad (10)$$

and,

$$T_{\infty} = A_S + B_S \quad (11)$$

$$T_F = A_S + B_S \left\{ \operatorname{erfc}(\varphi) - \exp \left(\frac{h s}{k_S} + \frac{h^2 s^2}{4\varphi^2 k_S^2} \right) \operatorname{erfc} \left(\varphi + \frac{h s}{2\varphi k_S} \right) \right\} \quad (12)$$

Subtracting Eq. (12) from Eq. (11) leads to

$$T_{\infty} - T_F = B_S \left\{ 1 - \operatorname{erfc}(\varphi) + \exp \left(\frac{h s}{k_S} + \frac{h^2 s^2}{4\varphi^2 k_S^2} \right) \operatorname{erfc} \left(\varphi + \frac{h s}{2\varphi k_S} \right) \right\} \quad (13)$$

which gives B_S as

$$B_S = \frac{T_\infty - T_F}{\left\{1 - \operatorname{erfc}(\varphi) + \exp\left(\frac{h s}{k_S} + \frac{h^2 s^2}{4\varphi^2 k_S^2}\right) \operatorname{erfc}\left(\varphi + \frac{h s}{2\varphi k_S}\right)\right\}} \quad (14)$$

Similarly, the constant A_S can be determined as follows:

$$A_S = T_F - \frac{(T_\infty - T_F)}{\left\{1 - \operatorname{erfc}(\varphi) + \exp\left(\frac{h s}{k_S} + \frac{h^2 s^2}{4\varphi^2 k_S^2}\right) \operatorname{erfc}\left(\varphi + \frac{h s}{2\varphi k_S}\right)\right\}} \left\{ \operatorname{erfc}(\varphi) - \exp\left(\frac{h s}{k_S} + \frac{h^2 s^2}{4\varphi^2 k_S^2}\right) \operatorname{erfc}\left(\varphi + \frac{h s}{2\varphi k_S}\right) \right\} \quad (15)$$

The temperature profile can now be expressed in terms of constant A_S and B_S ,

$$\begin{aligned} & \frac{T_S(x, t) - T_F}{T_\infty - T_F} \\ &= \frac{\left\{ \operatorname{erfc}\left(\frac{x}{2\sqrt{\alpha_S t}}\right) - \exp\left(\frac{h x}{k_S} + \frac{h^2 \alpha_S t}{k_S^2}\right) \operatorname{erfc}\left(\frac{x}{2\sqrt{\alpha_S t}} + \frac{h \sqrt{\alpha_S t}}{k_S}\right) - \operatorname{erfc}(\varphi) + \exp\left(\frac{h s}{k_S} + \frac{h^2 s^2}{4\varphi^2 k_S^2}\right) \operatorname{erfc}\left(\varphi + \frac{h s}{2\varphi k_S}\right) \right\}}{\left\{1 - \operatorname{erfc}(\varphi) + \exp\left(\frac{h s}{k_S} + \frac{h^2 s^2}{4\varphi^2 k_S^2}\right) \operatorname{erfc}\left(\varphi + \frac{h s}{2\varphi k_S}\right)\right\}} \end{aligned} \quad (16)$$

Aiming to express the temperature profile in a more suitable form, the following auxiliary functions $\psi(s, \varphi)$ and $\zeta(s, \varphi)$ can be defined as

$$\psi(s, t) = \left\{1 - \operatorname{erfc}(\varphi) + \exp\left(\frac{h s}{k_S} + \frac{h^2 \alpha_S t}{k_S^2}\right) \operatorname{erfc}\left(\varphi + \frac{h \sqrt{\alpha_S t}}{k_S}\right)\right\} \quad (17a)$$

$$\psi(s, \varphi) = \left\{1 - \operatorname{erfc}(\varphi) + \exp\left(\frac{h s}{k_S} + \frac{h^2 s^2}{4\varphi^2 k_S^2}\right) \operatorname{erfc}\left(\varphi + \frac{h s}{2\varphi k_S}\right)\right\} \quad (17b)$$

and,

$$\zeta(s, t) = -\operatorname{erfc}(\varphi) + \exp\left(\frac{h s}{k_S} + \frac{h^2 \alpha_S t}{k_S^2}\right) \operatorname{erfc}\left(\varphi + \frac{h \sqrt{\alpha_S t}}{k_S}\right) \quad (18a)$$

$$\zeta(s, \varphi) = -\operatorname{erfc}(\varphi) + \exp\left(\frac{h s}{k_S} + \frac{h^2 s^2}{4\varphi^2 k_S^2}\right) \operatorname{erfc}\left(\varphi + \frac{h s}{2\varphi k_S}\right) \quad (18b)$$

Substituting Eq. (17) and Eq. (18) into Eq. (16) yields

$$\frac{T_S(x, t) - T_F}{T_\infty - T_F} = \frac{\left\{ \operatorname{erfc}\left(\frac{x}{2\sqrt{\alpha_S t}}\right) - \exp\left(\frac{h x}{k_S} + \frac{h^2 \alpha_S t}{k_S^2}\right) \operatorname{erfc}\left(\frac{x}{2\sqrt{\alpha_S t}} + \frac{h \sqrt{\alpha_S t}}{k_S}\right) + \zeta(s, t) \right\}}{\psi(s, t)} \quad (19a)$$

$$\frac{T_S(x, s) - T_F}{T_\infty - T_F} = \frac{\left\{ \operatorname{erfc}\left(\frac{x}{2\sqrt{\alpha_S t}}\right) - \exp\left(\frac{h x}{k_S} + \frac{h^2 \alpha_S t}{k_S^2}\right) \operatorname{erfc}\left(\frac{x}{2\sqrt{\alpha_S t}} + \frac{h \sqrt{\alpha_S t}}{k_S}\right) + \zeta(s, \varphi) \right\}}{\psi(s, \varphi)} \quad (19b)$$

The thermal gradient $T_S(x, t)$ in the vicinity of boundary $x = -s$ is found by deriving the temperature profile with respect to x , which has the following form:

$$\begin{aligned} & \frac{\partial T_S(s, t)}{\partial x} \Big|_{x=-s} = \frac{(T_F - T_\infty)}{\psi(s, t)} \left\{ \frac{h}{k_S} \exp\left(\frac{h s}{k_S} + \frac{h^2 \alpha_S t}{k_S^2}\right) \exp\left(\varphi + \frac{h \sqrt{\alpha_S t}}{k_S}\right) + \frac{2\varphi}{\sqrt{\pi s} \exp(\varphi^2)} - \frac{2\varphi}{\sqrt{\pi s} \exp\left[\left(\varphi + \frac{h \sqrt{\alpha_S t}}{k_S}\right)^2\right]} \exp\left(\frac{h s}{k_S} + \right. \right. \\ & \left. \left. \frac{h^2 \alpha_S t}{k_S^2}\right) \right\} \end{aligned} \quad (20a)$$

$$\left. \frac{\partial T_S(s, \varphi)}{\partial x} \right|_{x=-s} = \frac{(T_F - T_\infty)}{\psi(s, \varphi)} \left\{ \frac{h}{k_S} \exp\left(\frac{h s}{k_S} + \frac{h^2 s^2}{4 \varphi^2 k_S^2}\right) \operatorname{erfc}\left(\varphi + \frac{h s}{2 \varphi k_S}\right) + \frac{2 \varphi}{\sqrt{\pi} s \exp(\varphi^2)} - \frac{2 \varphi}{\sqrt{\pi} s \exp\left[\left(\varphi + \frac{h s}{2 \varphi k_S}\right)^2\right]} \exp\left(\frac{h s}{k_S} + \frac{h^2 s^2}{4 \varphi^2 k_S^2}\right) \right\} \quad (20b)$$

A common way to write a solution of a partial differential equation to avoid instability concerning the magnitude of the involved dimensional variables in the function evaluation is to express this in terms of dimensionless numbers with physical meaning, such as Ste, Biot and Biot²Fo,

$$t = \frac{s^2}{4 \alpha_S \varphi^2} \quad (21)$$

$$Fo = \frac{\alpha_S t}{s^2} \quad (22)$$

$$Biot = \frac{h s}{k_S} \quad (23)$$

$$Ste = \frac{C_{PS}(T_F - T_\infty)}{L} \quad (24)$$

$$Biot^2 Fo = \frac{h^2 s^2}{4 \varphi^2 k_S^2} = \frac{Biot^2}{4 \varphi^2} \quad (25)$$

$$\psi(Biot, \varphi) = \left\{ 1 - \operatorname{erfc}(\varphi) + \exp\left(Biot + \frac{Biot^2}{4 \varphi^2}\right) \operatorname{erfc}\left(\varphi + \frac{Biot}{2 \varphi}\right) \right\} \quad (26)$$

The derivative of s with respect to t gives

$$\frac{ds}{dt} = \frac{2 \varphi^2 \alpha_S}{s} \quad (27)$$

and by substituting the temperature gradient $\left. \frac{\partial T_S(x, t)}{\partial x} \right|_{x=-s}$ into the moving boundary heat balance, Eq. (26), the similarity root φ can be obtained as

$$\rho_S L \frac{2 \varphi^2 \alpha_S}{s} = k_S \frac{(T_F - T_\infty)}{\psi(s, \varphi)} \left\{ \frac{h}{k_S} \exp\left(\frac{h s}{k_S} + \frac{h^2 s^2}{4 \varphi^2 k_S^2}\right) \operatorname{erfc}\left(\varphi + \frac{h s}{2 \varphi k_S}\right) + \frac{2 \varphi}{\sqrt{\pi} s \exp(\varphi^2)} - \frac{2 \varphi}{\sqrt{\pi} s \exp\left[\left(\varphi + \frac{h s}{2 \varphi k_S}\right)^2\right]} \exp\left(\frac{h s}{k_S} + \frac{h^2 s^2}{4 \varphi^2 k_S^2}\right) \right\} \quad (28)$$

Eq. (28) is rearranged to the following form:

$$\varphi \frac{L}{C_{PS}(T_F - T_\infty)} = \frac{1}{\psi(s, \varphi)} \left\{ \frac{h s}{2 \varphi k_S} \exp\left(\frac{h s}{k_S} + \frac{h^2 s^2}{4 \varphi^2 k_S^2}\right) \operatorname{erfc}\left(\varphi + \frac{h s}{2 \varphi k_S}\right) + \frac{1}{\sqrt{\pi} \exp(\varphi^2)} - \frac{1}{\sqrt{\pi} \exp\left[\left(\varphi + \frac{h s}{2 \varphi k_S}\right)^2\right]} \exp\left(\frac{h s}{k_S} + \frac{h^2 s^2}{4 \varphi^2 k_S^2}\right) \right\} \quad (29)$$

Eq. (29), expressed in terms of dimensionless numbers and parameters of heat conduction, becomes

$$\varphi = \frac{Ste}{\psi(Biot, \varphi)} \left\{ \frac{Biot}{2 \varphi} \exp\left(Biot + \frac{Biot^2}{4 \varphi^2}\right) \operatorname{erfc}\left(\varphi + \frac{Biot}{2 \varphi}\right) + \frac{1}{\sqrt{\pi} \exp(\varphi^2)} - \frac{1}{\sqrt{\pi} \exp\left[\left(\varphi + \frac{Biot}{2 \varphi}\right)^2\right]} \exp\left(Biot + \frac{Biot^2}{4 \varphi^2}\right) \right\} \quad (30)$$

Similarly, the temperature profile $\theta_s(x, t) = \frac{T_s(x, t) - T_F}{T_\infty - T_F}$ and the auxiliary function $\zeta(s, \varphi)$ can be written as a function of *Biot* and the interface position *s* according to the following expressions:

$$\frac{T_s(x, s) - T_F}{T_\infty - T_F} = \frac{\left\{ \operatorname{erfc}\left(\varphi \frac{x}{s}\right) - \exp\left(\operatorname{Biot} \frac{x}{s} + \frac{\operatorname{Biot}^2}{4\varphi^2}\right) \operatorname{erfc}\left(\varphi \frac{x}{s} + \frac{\operatorname{Biot}}{2\varphi}\right) + \zeta(\operatorname{Biot}, \varphi) \right\}}{\psi(\operatorname{Biot}, \varphi)} \quad (31)$$

and

$$\zeta(\operatorname{Biot}, \varphi) = -\operatorname{erfc}(\varphi) + \exp\left(\operatorname{Biot} + \frac{\operatorname{Biot}^2}{4\varphi^2}\right) \operatorname{erfc}\left(\varphi + \frac{\operatorname{Biot}}{2\varphi}\right) \quad (32)$$

Wagner, cited by Jost [59], assumed tentatively that the plane of discontinuity is shifted proportionally with \sqrt{t} when analysing one-phase solid-state diffusion, which is valid only for high Biot numbers. In the present study, the relationship between the position of the interface and time is better posed by a combination of parabolic and linear profiles, whose linear profile represents the ratio between any position *s* and the *Biot* related to the material diffusion capacity $\frac{h\alpha_s t}{k_s}$, i.e., dimensional

$$t = \frac{s^2}{4\alpha_s \varphi^2} + \frac{2 s k_s \varphi}{h \alpha_s} \quad (33a)$$

and dimensionless time,

$$t^* = \frac{s^{*2}}{4 Fo \varphi^2} + \frac{2 s^* \varphi}{\operatorname{Biot} Fo} \quad (33b)$$

Three-dimensional One-Phase Moving Boundary Problem

A three-dimensional one-phase transient solution for the freezing/solidification of a semi-infinite slab can be described by the PDE in Eq. (34), the initial Eq. (35)-(37), and the boundary conditions Eq. (38)-(46) as follows:

$$\frac{\partial^2 T_s}{\partial x^2} + \frac{\partial^2 T_s}{\partial y^2} + \frac{\partial^2 T_s}{\partial z^2} = \frac{1}{\alpha_s} \frac{\partial T_s}{\partial t}, \quad 0 < x < s_x(t), \quad 0 < y < s_y(t), \text{ and } 0 < z < s_z(t) \quad (34)$$

$$t = 0, \quad 0 < x < +\infty, \quad T_s = T_F \quad (35)$$

$$t = 0, \quad 0 < y < +\infty, \quad T_s = T_F \quad (36)$$

$$t = 0, \quad 0 < z < +\infty, \quad T_s = T_F \quad (37)$$

$$t > 0, \quad x = 0, \quad h_x(T - T_{\infty_x}) = -k_{s_x} \left. \frac{\partial T_s}{\partial x} \right|_{x=0} \quad (38)$$

$$t > 0, \quad y = 0, \quad h_y(T - T_{\infty_y}) = -k_{s_y} \left. \frac{\partial T_s}{\partial y} \right|_{y=0} \quad (39)$$

$$t > 0, \quad z = 0, \quad h_z(T - T_{\infty_z}) = -k_{s_z} \left. \frac{\partial T_s}{\partial z} \right|_{z=0} \quad (40)$$

$$t > 0, \quad x = s_x(t), \quad T_s = T_F \quad (41)$$

$$t > 0, \quad y = s_y(t), \quad T_s = T_F \quad (42)$$

$$t > 0, \quad z = s_z(t), \quad T_s = T_F \quad (43)$$

$$t > 0, \quad x \rightarrow +\infty, \quad T_s = T_F \quad (44)$$

$$t > 0, \quad y \rightarrow +\infty, \quad T_s = T_F \quad (45)$$

$$t > 0, \quad z \rightarrow +\infty, \quad T_s = T_F \quad (46)$$

$$\rho_s L \frac{ds}{dt} = k_{s_x} \left. \frac{\partial T_s}{\partial x} \right|_{x=-s_x} + k_{s_y} \left. \frac{\partial T_s}{\partial y} \right|_{y=-s_y} + k_{s_z} \left. \frac{\partial T_s}{\partial z} \right|_{z=-s_z} \quad (47)$$

where $\vec{s} = \hat{i}s_x + \hat{j}s_y + \hat{k}s_z$, $\vec{\rho}_s = \hat{i}\rho_{s_x} + \hat{j}\rho_{s_y} + \hat{k}\rho_{s_z}$, $\vec{k}_s = \hat{i}k_{s_x} + \hat{j}k_{s_y} + \hat{k}k_{s_z}$ and $\vec{C}_{ps} = \hat{i}C_{ps_x} + \hat{j}C_{ps_y} + \hat{k}C_{ps_z}$. A three-dimensional solution for the temperature profile can be considered as the product of the solutions in x , y and z axes, that is,

$$\theta(x, y, z, t) = \theta_x(x, t) \cdot \theta_y(y, t) \cdot \theta_z(z, t) \quad (48)$$

which, in terms of $\frac{T_S(x, y, z, t) - T_F}{T_{\infty_i} - T_F}$ gives

$$\frac{T_S(x, y, z, t) - T_F}{T_{\infty_i} - T_F} = \left[\frac{T_S(x, t) - T_F}{T_{\infty_x} - T_F} \right] \cdot \left[\frac{T_S(y, t) - T_F}{T_{\infty_y} - T_F} \right] \cdot \left[\frac{T_S(z, t) - T_F}{T_{\infty_z} - T_F} \right] \quad (49)$$

The solutions for the temperature profiles x , y , and z are designated as

$$\frac{T_S(x, t) - T_F}{T_{\infty_x} - T_F} = \frac{\left\{ \operatorname{erfc} \left(\frac{x}{2\sqrt{\alpha_{s_x} t}} \right) - \exp \left(\frac{h_x x}{k_{s_x}} + \frac{h_x^2 \alpha_{s_x} t}{k_{s_x}^2} \right) \operatorname{erfc} \left(\frac{x}{2\sqrt{\alpha_{s_x} t}} + \frac{h_x \sqrt{\alpha_{s_x} t}}{k_{s_x}} \right) + \zeta(s_x, \varphi) \right\}}{\psi(s_x, \varphi)} \quad (50)$$

$$\frac{T_S(y, t) - T_F}{T_{\infty_y} - T_F} = \frac{\left\{ \operatorname{erfc} \left(\frac{y}{2\sqrt{\alpha_{s_y} t}} \right) - \exp \left(\frac{h_y y}{k_{s_y}} + \frac{h_y^2 \alpha_{s_y} t}{k_{s_y}^2} \right) \operatorname{erfc} \left(\frac{y}{2\sqrt{\alpha_{s_y} t}} + \frac{h_y \sqrt{\alpha_{s_y} t}}{k_{s_y}} \right) + \zeta(s_y, \varphi) \right\}}{\psi(s_y, \varphi)} \quad (51)$$

$$\frac{T_S(z, t) - T_F}{T_{\infty_z} - T_F} = \frac{\left\{ \operatorname{erfc} \left(\frac{z}{2\sqrt{\alpha_{s_z} t}} \right) - \exp \left(\frac{h_z z}{k_{s_z}} + \frac{h_z^2 \alpha_{s_z} t}{k_{s_z}^2} \right) \operatorname{erfc} \left(\frac{z}{2\sqrt{\alpha_{s_z} t}} + \frac{h_z \sqrt{\alpha_{s_z} t}}{k_{s_z}} \right) + \zeta(s_z, \varphi) \right\}}{\psi(s_z, \varphi)} \quad (52)$$

By making $i = \{x, y, z\}$ and writing the auxiliary functions $\psi(s_i, \varphi)$ and $\zeta(s_i, \varphi)$ in terms of i , result in

$$\psi(s_i, t) = \left\{ 1 - \operatorname{erfc}(\varphi) + \exp \left(\frac{h_i s_i}{k_{s_i}} + \frac{h_i^2 \alpha_{s_i} t}{k_{s_i}^2} \right) \operatorname{erfc} \left(\varphi + \frac{h_i \sqrt{\alpha_{s_i} t}}{k_{s_i}} \right) \right\} \quad (53a)$$

$$\psi(s_i, \varphi) = \left\{ 1 - \operatorname{erfc}(\varphi) + \exp \left(\frac{h_i s_i}{k_{s_i}} + \frac{h_i^2 s_i^2}{4\varphi^2 k_{s_i}^2} \right) \operatorname{erfc} \left(\varphi + \frac{h_i s_i}{2\varphi k_{s_i}} \right) \right\} \quad (53b)$$

and,

$$\zeta(s_i, t) = -\operatorname{erfc}(\varphi) + \exp \left(\frac{h_i s_i}{k_{s_i}} + \frac{h_i^2 \alpha_{s_i} t}{k_{s_i}^2} \right) \operatorname{erfc} \left(\varphi + \frac{h_i \sqrt{\alpha_{s_i} t}}{k_{s_i}} \right) \quad (54a)$$

$$\zeta(s_i, \varphi) = -\operatorname{erfc}(\varphi) + \exp \left(\frac{h_i s_i}{k_{s_i}} + \frac{h_i^2 s_i^2}{4\varphi^2 k_{s_i}^2} \right) \operatorname{erfc} \left(\varphi + \frac{h_i s_i}{2\varphi k_{s_i}} \right) \quad (54b)$$

By writing Eq. (50)-(52) as a function of position s through the similarity variable $\varphi = \frac{s}{2\sqrt{\alpha_{s_i} t}}$, the derivatives of the temperature profile at $x = -s_x$, $y = -s_y$ and $z = -s_z$ are

$$\left. \frac{\partial T_S(s,t)}{\partial x} \right|_{x=-s_x} = \frac{(T_F - T_{\infty_x})}{\psi(s_x, t)} \left\{ \frac{h_x}{k_{S_x}} \exp\left(\frac{h_x s_x}{k_{S_x}} + \frac{h_x^2 \alpha_{S_x} t}{k_{S_x}^2}\right) \exp\left(\varphi + \frac{h_x \sqrt{\alpha_{S_x} t}}{k_{S_x}}\right) + \frac{2\varphi}{\sqrt{\pi} s_x \exp(\varphi^2)} - \frac{2\varphi}{\sqrt{\pi} s_x \exp\left[\left(\varphi + \frac{h_x \sqrt{\alpha_{S_x} t}}{k_{S_x}}\right)^2\right]} \exp\left(\frac{h_x s_x}{k_{S_x}} + \frac{h_x^2 \alpha_{S_x} t}{k_{S_x}^2}\right) \right\}$$

(55a)

$$\left. \frac{\partial T_S(x,t)}{\partial x} \right|_{x=-s_x} = \frac{(T_F - T_{\infty_x})}{\psi(s_x, \varphi)} \left\{ \frac{h_x}{k_{S_x}} \exp\left(\frac{h_x s_x}{k_{S_x}} + \frac{h_x^2 s_x^2}{4 \varphi^2 k_{S_x}^2}\right) \exp\left(\varphi + \frac{h_x s_x}{2 \varphi k_{S_x}}\right) + \frac{2\varphi}{\sqrt{\pi} s_x \exp(\varphi^2)} - \frac{2\varphi}{\sqrt{\pi} s_x \exp\left[\left(\varphi + \frac{h_x s_x}{2 \varphi k_{S_x}}\right)^2\right]} \exp\left(\frac{h_x s_x}{k_{S_x}} + \frac{h_x^2 s_x^2}{4 \varphi^2 k_{S_x}^2}\right) \right\}$$

(55b)

$$\left. \frac{\partial T_S(s,t)}{\partial y} \right|_{y=-s_y} = \frac{(T_F - T_{\infty_y})}{\psi(s_y, t)} \left\{ \frac{h_y}{k_{S_y}} \exp\left(\frac{h_y s_y}{k_{S_y}} + \frac{h_y^2 \alpha_{S_y} t}{k_{S_y}^2}\right) \exp\left(\varphi + \frac{h_y \sqrt{\alpha_{S_y} t}}{k_{S_y}}\right) + \frac{2\varphi}{\sqrt{\pi} s_y \exp(\varphi^2)} - \frac{2\varphi}{\sqrt{\pi} s_y \exp\left[\left(\varphi + \frac{h_y \sqrt{\alpha_{S_y} t}}{k_{S_y}}\right)^2\right]} \exp\left(\frac{h_y s_y}{k_{S_y}} + \frac{h_y^2 \alpha_{S_y} t}{k_{S_y}^2}\right) \right\}$$

(56a)

$$\left. \frac{\partial T_S(y,t)}{\partial y} \right|_{y=-s_y} = \frac{(T_F - T_y)}{\psi(s_y, \varphi)} \left\{ \frac{h_y}{k_{S_y}} \exp\left(\frac{h_y s_y}{k_{S_y}} + \frac{h_y^2 s_y^2}{4 \varphi^2 k_{S_y}^2}\right) \exp\left(\varphi + \frac{h_y s_y}{2 \varphi k_{S_y}}\right) + \frac{2\varphi}{\sqrt{\pi} s_y \exp(\varphi^2)} - \frac{2\varphi}{\sqrt{\pi} s_y \exp\left[\left(\varphi + \frac{h_y s_y}{2 \varphi k_{S_y}}\right)^2\right]} \exp\left(\frac{h_y s_y}{k_{S_y}} + \frac{h_y^2 s_y^2}{4 \varphi^2 k_{S_y}^2}\right) \right\}$$

(56b)

$$\left. \frac{\partial T_S(s,t)}{\partial z} \right|_{z=-s_z} = \frac{(T_F - T_{\infty_z})}{\psi(s_z, t)} \left\{ \frac{h_z}{k_{S_z}} \exp\left(\frac{h_z s_z}{k_{S_z}} + \frac{h_z^2 \alpha_{S_z} t}{k_{S_z}^2}\right) \exp\left(\varphi + \frac{h_z \sqrt{\alpha_{S_z} t}}{k_{S_z}}\right) + \frac{2\varphi}{\sqrt{\pi} s_z \exp(\varphi^2)} - \frac{2\varphi}{\sqrt{\pi} s_z \exp\left[\left(\varphi + \frac{h_z \sqrt{\alpha_{S_z} t}}{k_{S_z}}\right)^2\right]} \exp\left(\frac{h_z s_z}{k_{S_z}} + \frac{h_z^2 \alpha_{S_z} t}{k_{S_z}^2}\right) \right\}$$

(57a)

$$\left. \frac{\partial T_S(z,t)}{\partial z} \right|_{z=-s_z} = \frac{(T_F - T_z)}{\psi(s_z, \varphi)} \left\{ \frac{h_z}{k_{S_z}} \exp\left(\frac{h_z s_z}{k_{S_z}} + \frac{h_z^2 s_z^2}{4 \varphi^2 k_{S_z}^2}\right) \exp\left(\varphi + \frac{h_z s_z}{2 \varphi k_{S_z}}\right) + \frac{2\varphi}{\sqrt{\pi} s_z \exp(\varphi^2)} - \frac{2\varphi}{\sqrt{\pi} s_z \exp\left[\left(\varphi + \frac{h_z s_z}{2 \varphi k_{S_z}}\right)^2\right]} \exp\left(\frac{h_z s_z}{k_{S_z}} + \frac{h_z^2 s_z^2}{4 \varphi^2 k_{S_z}^2}\right) \right\}$$

(57b)

The similarity variable is applied here to determine its derivative to express the dependence of the transformation interface velocity on s , as shown by Eq. (57):

$$\frac{ds}{dt} = \frac{2\varphi^2 \alpha_s}{s} \quad (58)$$

By inserting the temperature gradients into the heat balance in the moving transformation interface, as shown in Eq. (47), the similarity variable can be determined as follows:

$$\varphi = \frac{C_{PS_x}(T_F - T_{\infty_x})}{L_x \psi_x(s_x, \varphi)} \left\{ \frac{h_x s_x}{2\varphi k_{S_x}} \exp\left(\frac{h_x s_x}{k_{S_x}} + \frac{h_x^2 s_x^2}{4\varphi^2 k_{S_x}^2}\right) \operatorname{erfc}\left(\varphi + \frac{h_x s_x}{2\varphi k_{S_x}}\right) + \frac{1}{\sqrt{\pi} \exp(\varphi^2)} - \frac{1}{\sqrt{\pi} \exp\left[\left(\varphi + \frac{h_x s_x}{2\varphi k_{S_x}}\right)^2\right]} \exp\left(\frac{h_x s_x}{k_{S_x}} + \frac{h_x^2 s_x^2}{4\varphi^2 k_{S_x}^2}\right) \right. \\ \left. \frac{h_x s_x}{k_{S_x}} + \frac{h_x^2 s_x^2}{4\varphi^2 k_{S_x}^2} + \frac{C_{PS_y}(T_F - T_{\infty_y})}{L_y \psi_y(s_y, \varphi)} \left\{ \frac{h_y s_y}{2\varphi k_{S_y}} \exp\left(\frac{h_y s_y}{k_{S_y}} + \frac{h_y^2 s_y^2}{4\varphi^2 k_{S_y}^2}\right) \operatorname{erfc}\left(\varphi + \frac{h_y s_y}{2\varphi k_{S_y}}\right) + \frac{1}{\sqrt{\pi} \exp(\varphi^2)} - \frac{1}{\sqrt{\pi} \exp\left[\left(\varphi + \frac{h_y s_y}{2\varphi k_{S_y}}\right)^2\right]} \exp\left(\frac{h_y s_y}{k_{S_y}} + \frac{h_y^2 s_y^2}{4\varphi^2 k_{S_y}^2}\right) \right\} \right. \\ \left. \frac{h_z s_z}{k_{S_z}} + \frac{h_z^2 s_z^2}{4\varphi^2 k_{S_z}^2} + \frac{C_{PS_z}(T_F - T_{\infty_z})}{L_z \psi_z(s_z, \varphi)} \left\{ \frac{h_z s_z}{2\varphi k_{S_z}} \exp\left(\frac{h_z s_z}{k_{S_z}} + \frac{h_z^2 s_z^2}{4\varphi^2 k_{S_z}^2}\right) \operatorname{erfc}\left(\varphi + \frac{h_z s_z}{2\varphi k_{S_z}}\right) + \frac{1}{\sqrt{\pi} \exp(\varphi^2)} - \frac{1}{\sqrt{\pi} \exp\left[\left(\varphi + \frac{h_z s_z}{2\varphi k_{S_z}}\right)^2\right]} \exp\left(\frac{h_z s_z}{k_{S_z}} + \frac{h_z^2 s_z^2}{4\varphi^2 k_{S_z}^2}\right) \right\} \right\} \quad (59)$$

By writing the expressions for the temperature profile in each direction and auxiliary functions $\psi(s_i, \varphi)$ and $\zeta(s_i, \varphi)$ in relation to Ste_i , $Biot_i$, and $Biot_i^2 Fo_i$ dimensionless numbers,

$$t = \frac{s^2}{4\alpha_s \varphi^2} = \frac{s_x^2 + s_y^2 + s_z^2}{4\sqrt{\alpha_s^2 + \alpha_{S_y}^2 + \alpha_{S_z}^2} \varphi^2} \quad (60)$$

$$Fo_i = \frac{\alpha_{S_i} t}{s_i^2} \quad (61)$$

$$Biot_i = \frac{h_i s_i}{k_{S_i}} \quad (62)$$

$$Ste_i = \frac{C_{PS_i}(T_F - T_{\infty_i})}{L_i} \quad (63)$$

$$Biot_i^2 Fo_i = \frac{h_i^2 s_i^2}{4\varphi^2 k_{S_i}^2} = \frac{Biot_i^2}{4\varphi^2} \quad (64)$$

In this case, the functions $\psi(s_i, \varphi)$ are given by

$$\psi(Biot_x, \varphi) = \left\{ 1 - \operatorname{erfc}(\varphi) + \exp\left(Biot_x + \frac{Biot_x^2}{4\varphi^2}\right) \operatorname{erfc}\left(\varphi + \frac{Biot_x}{2\varphi}\right) \right\} \quad (65)$$

$$\psi(Biot_y, \varphi) = \left\{ 1 - \operatorname{erfc}(\varphi) + \exp\left(Biot_y + \frac{Biot_y^2}{4\varphi^2}\right) \operatorname{erfc}\left(\varphi + \frac{Biot_y}{2\varphi}\right) \right\} \quad (66)$$

$$\psi(Biot_z, \varphi) = \left\{ 1 - \operatorname{erfc}(\varphi) + \exp\left(Biot_z + \frac{Biot_z^2}{4\varphi^2}\right) \operatorname{erfc}\left(\varphi + \frac{Biot_z}{2\varphi}\right) \right\} \quad (67)$$

Similarly, the functions $\zeta(s_i, \varphi)$ in the corresponding directions are

$$\zeta(\text{Biot}_x, \varphi) = -\text{erfc}(\varphi) + \exp\left(\text{Biot}_x + \frac{\text{Biot}_x^2}{4\varphi^2}\right) \text{erfc}\left(\varphi + \frac{\text{Biot}_x}{2\varphi}\right) \quad (68)$$

$$\zeta(\text{Biot}_y, \varphi) = -\text{erfc}(\varphi) + \exp\left(\text{Biot}_y + \frac{\text{Biot}_y^2}{4\varphi^2}\right) \text{erfc}\left(\varphi + \frac{\text{Biot}_y}{2\varphi}\right) \quad (69)$$

$$\zeta(\text{Biot}_z, \varphi) = -\text{erfc}(\varphi) + \exp\left(\text{Biot}_z + \frac{\text{Biot}_z^2}{4\varphi^2}\right) \text{erfc}\left(\varphi + \frac{\text{Biot}_z}{2\varphi}\right) \quad (70)$$

Then, by writing Eq. (59) as a function of the dimensionless heat conduction number, we obtain

$$\varphi = \frac{\text{Ste}_x}{\psi(\text{Biot}_x, \varphi)} \left\{ \frac{\text{Biot}_x}{2\varphi} \exp\left(\text{Biot}_x + \frac{\text{Biot}_x^2}{4\varphi^2}\right) \text{erfc}\left(\varphi + \frac{\text{Biot}_x}{2\varphi}\right) + \frac{1}{\sqrt{\pi} \exp(\varphi^2)} - \frac{1}{\sqrt{\pi} \exp\left[\left(\varphi + \frac{\text{Biot}_x}{2\varphi}\right)^2\right]} \exp\left(\text{Biot}_x + \frac{\text{Biot}_x^2}{4\varphi^2}\right) \right\} \quad (71)$$

Similarly, for the temperature profiles for the three axes,

$$\theta_x(x, s_x) = \frac{T_S(x, s_x) - T_F}{T_{\infty x} - T_F} = \frac{\left\{ \text{erfc}\left(\varphi \frac{x}{s_x}\right) - \exp\left(\text{Biot}_x \frac{x}{s_x} + \frac{\text{Biot}_x^2}{4\varphi^2}\right) \text{erfc}\left(\varphi \frac{x}{s_x} + \frac{\text{Biot}_x}{2\varphi}\right) + \zeta_x(\text{Biot}_x, \varphi) \right\}}{\psi_x(\text{Biot}_x, \varphi)} \quad (72)$$

for $\theta_y(y, s_y)$,

$$\theta_y(y, s_y) = \frac{T_S(y, s_y) - T_F}{T_{\infty y} - T_F} = \frac{\left\{ \text{erfc}\left(\varphi \frac{y}{s_y}\right) - \exp\left(\text{Biot}_y \frac{y}{s_y} + \frac{\text{Biot}_y^2}{4\varphi^2}\right) \text{erfc}\left(\varphi \frac{y}{s_y} + \frac{\text{Biot}_y}{2\varphi}\right) + \zeta_y(\text{Biot}_y, \varphi) \right\}}{\psi_y(\text{Biot}_y, \varphi)} \quad (73)$$

and for $\theta_z(z, s_z)$

$$\theta_z(z, s_z) = \frac{T_S(z, s_z) - T_F}{T_{\infty z} - T_F} = \frac{\left\{ \text{erfc}\left(\varphi \frac{z}{s_z}\right) - \exp\left(\text{Biot}_z \frac{z}{s_z} + \frac{\text{Biot}_z^2}{4\varphi^2}\right) \text{erfc}\left(\varphi \frac{z}{s_z} + \frac{\text{Biot}_z}{2\varphi}\right) + \zeta_z(\text{Biot}_z, \varphi) \right\}}{\psi_z(\text{Biot}_z, \varphi)} \quad (74)$$

Finally, the three-dimensional solution for the temperature profile can be given by

$$\theta_S(x, y, z, s_x, s_y, s_z) = \theta_x(x, s_x) \theta_y(y, s_y) \theta_z(z, s_z) \quad (75)$$

that is,

$$\begin{aligned} \theta_S(x, y, z, s_x, s_y, s_z) &= \left[\frac{T_S(x, y, z, s_x, s_y, s_z) - T_F}{T_{\infty_i} - T_F} \right] = \theta_x(x, s_x) \theta_y(y, s_y) \theta_z(z, s_z) \\ &= \left[\frac{T_S(x, s_x) - T_F}{T_{\infty x} - T_F} \right] \left[\frac{T_S(y, s_y) - T_F}{T_{\infty y} - T_F} \right] \left[\frac{T_S(z, s_z) - T_F}{T_{\infty z} - T_F} \right] \\ &= \frac{\left\{ \text{erfc}\left(\varphi \frac{x}{s_x}\right) - \exp\left(\text{Biot}_x \frac{x}{s_x} + \frac{\text{Biot}_x^2}{4\varphi^2}\right) \text{erfc}\left(\varphi \frac{x}{s_x} + \frac{\text{Biot}_x}{2\varphi}\right) + \zeta_x(\text{Biot}_x, \varphi) \right\}}{\psi(\text{Biot}_x, \varphi)} \\ &\quad \frac{\left\{ \text{erfc}\left(\varphi \frac{y}{s_y}\right) - \exp\left(\text{Biot}_y \frac{y}{s_y} + \frac{\text{Biot}_y^2}{4\varphi^2}\right) \text{erfc}\left(\varphi \frac{y}{s_y} + \frac{\text{Biot}_y}{2\varphi}\right) + \zeta_y(\text{Biot}_y, \varphi) \right\}}{\psi(\text{Biot}_y, \varphi)} \end{aligned}$$

$$\frac{\left\{ \operatorname{erfc}\left(\varphi \frac{z}{s_z}\right) - \exp\left(\operatorname{Biot}_z \frac{z}{s_z} + \frac{\operatorname{Biot}_z^2}{4\varphi^2}\right) \operatorname{erfc}\left(\varphi \frac{z}{s_z} + \frac{\operatorname{Biot}_z}{2\varphi}\right) + \zeta_z(\operatorname{Biot}_z, \varphi) \right\}}{\psi(\operatorname{Biot}_z, \varphi)} \quad (76)$$

and the freezing/solidification time is given by the Biot number, which transitions from a parabolic to a linear profile and vice versa, posed as $\frac{s_i}{\frac{2h_i\alpha_{S_i}t}{k_{S_i}}}$ dimensional

$$t = t_x + t_y + t_z = \frac{s_x^2}{4\alpha_{S_x}\varphi^2} + \frac{s_y^2}{4\alpha_{S_y}\varphi^2} + \frac{s_z^2}{4\alpha_{S_z}\varphi^2} + \frac{2k_{S_x}s_x\varphi}{h_x\alpha_{S_x}} + \frac{2k_{S_y}s_y\varphi}{h_y\alpha_{S_y}} + \frac{2k_{S_z}s_z\varphi}{h_z\alpha_{S_z}} \quad (77a)$$

and dimensionless time,

$$t^* = \frac{s_x^{*2}}{4Fo_x\varphi^2} + \frac{s_y^{*2}}{4Fo_y\varphi^2} + \frac{s_z^{*2}}{4Fo_z\varphi^2} + \frac{2s_x^*\varphi}{\operatorname{Biot}_x Fo_x} + \frac{2s_y^*\varphi}{\operatorname{Biot}_y Fo_y} + \frac{2s_z^*\varphi}{\operatorname{Biot}_z Fo_z} \quad (77b)$$

One-dimensional Two-Phase Moving Boundary Problem

In the case of two-phase freezing/solidification of a pure or eutectic material with superheating in the liquid, as presented in Fig. 2, the governing partial differential equation and the initial and boundary conditions for a semi-infinite slab are given by

$$\frac{\partial^2 T_S}{\partial x^2} = \frac{1}{\alpha_S} \frac{\partial T_S}{\partial t} \quad 0 < x < s(t) \quad (78)$$

$$\frac{\partial^2 T_L}{\partial x^2} = \frac{1}{\alpha_L} \frac{\partial T_L}{\partial t} \quad s(t) < x < +\infty \quad (79)$$

$$t = 0, 0 < x < +\infty, \quad T = T_p \quad (80)$$

$$t > 0, x = 0, \quad -k \frac{\partial T}{\partial x} \Big|_{x=0} = h(T - T_\infty) \quad (81)$$

$$t > 0, x = s(t), \quad T = T_F \quad (82)$$

$$t > 0, x \rightarrow +\infty, \quad T = T_p \quad (83)$$

$$\rho_S L \frac{ds}{dt} = k_S \frac{\partial T_S}{\partial x} \Big|_{x=-s} - k_L \frac{\partial T_L}{\partial x} \Big|_{x=+s} \quad (84)$$

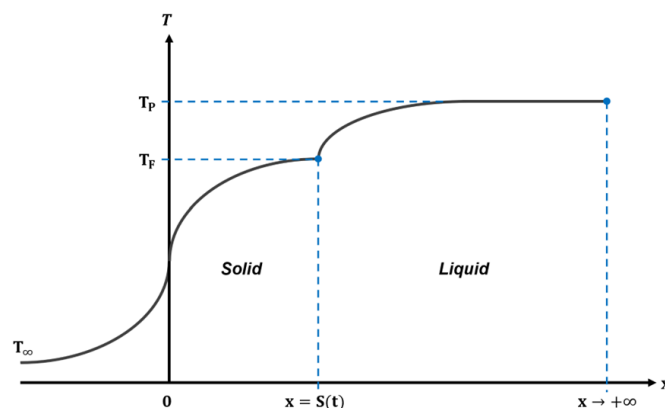


Figure 2 Schematic representation of two-phase transient solidification.

For the liquid phase, the proposed solution is given by

$$T_L(x, t) = A_L + B_L \left[1 - \operatorname{erf}\left(\frac{x}{2\sqrt{\alpha_L t}}\right) \right] \quad (85)$$

A relationship between the diffusivity of the solid and liquid phases is necessary to assess the similarity variable,

$$n = \sqrt{\frac{\alpha_S}{\alpha_L}} \quad (86)$$

Then, the solution becomes

$$T_L(x, t) = A_L + B_L \left[1 - \operatorname{erf}\left(\frac{nx}{2\sqrt{\alpha_S t}}\right) \right] \quad (87)$$

The substitution of initial and boundary conditions into the temperature profiles allows the constants A_L and B_L to be determined:

$$T_L(x = s(t), t) = T_F = A_L + B_L [1 - \operatorname{erf}(n\varphi)] \quad (88)$$

for A_L in $x \rightarrow +\infty$, when $t > 0$,

$$T_L(x \rightarrow +\infty, t) = T_P = A_L + 0 \therefore A_L = T_P \quad (89)$$

$$T_F = T_P + B_L [1 - \operatorname{erf}(n\varphi)] \quad (90)$$

The constant B_L can be determined as

$$B_L = \frac{T_F - T_P}{1 - \operatorname{erf}(n\varphi)} \quad (91)$$

Finally, after the substitution of constants in the liquid-phase temperature profile gives

$$T_L(x, t) = T_P + \frac{T_F - T_P}{1 - \operatorname{erf}(n\varphi)} \cdot \left[1 - \operatorname{erf}\left(\frac{nx}{2\sqrt{\alpha_S t}}\right) \right] \quad (92)$$

However, by knowing that,

$$\frac{1}{2\sqrt{\alpha_S t}} = \frac{\varphi}{s} \quad (93a)$$

and,

$$\frac{x}{2\sqrt{\alpha_S t}} = \varphi \frac{x}{s} \quad (93b)$$

and combining Eq. (93) and Eq. (92) results in

$$\frac{T_L(x, t) - T_P}{T_F - T_P} = \theta_L(x, t) = \frac{1}{1 - \operatorname{erf}(n\varphi)} \cdot \left[1 - \operatorname{erf}\left(\frac{nx}{2\sqrt{\alpha_S t}}\right) \right] \quad (94a)$$

$$\frac{T_L(x, s) - T_P}{T_F - T_P} = \theta_L(x, s) = \frac{1}{1 - \operatorname{erf}(n\varphi)} \cdot \left[1 - \operatorname{erf}\left(n\varphi \frac{x}{s}\right) \right] \quad (94b)$$

The derivative of $T_L(x, s)$ with respect to x at $x = s^+$ furnishes the temperature gradient for the liquid phase at the moving interface,

$$\left. \frac{\partial T_L}{\partial x} \right|_{x=s^+} = -\frac{1}{\sqrt{\pi}} \cdot \frac{T_P - T_F}{[1 - \operatorname{erf}(n\varphi)]} \cdot n \cdot \frac{1}{\sqrt{\alpha_S t}} \cdot \exp(-n^2 \varphi^2) \quad (95)$$

By inserting the similarity variable φ in Eq. (95),

$$\left. \frac{\partial T_L}{\partial x} \right|_{x=s^+} = -\frac{2\varphi n}{\sqrt{\pi} s} \cdot \frac{(T_P - T_F)}{\operatorname{erfc}(n\varphi)} \cdot \exp(-n^2 \varphi^2) \quad (96)$$

It is important to mention that sometimes the thermal gradient is a function of both the interface position and time, as presented in Eq. (97):

$$\left. \frac{\partial T_L}{\partial x} \right|_{x=s^+} = -\frac{2\varphi n}{\sqrt{\pi} s} \cdot \frac{(T_P - T_F)}{\operatorname{erfc}\left(n \frac{s}{2\sqrt{\alpha_S t}}\right)} \cdot \exp\left(-n^2 \frac{s^2}{4\alpha_S t}\right) \quad (97)$$

By combining Eq. (20), Eq. (27), Eq. (84), and Eq. (97), the similarity variable can be found:

$$\rho_S L \frac{2\varphi^2 \alpha_S}{s} = k_S \frac{(T_F - T_\infty)}{\psi(s, \varphi)} \left\{ \frac{h}{k_S} \exp\left(\frac{h s}{k_S} + \frac{h^2 s^2}{4 \varphi^2 k_S^2}\right) \operatorname{erfc}\left(\varphi + \frac{h s}{2 \varphi k_S}\right) + \frac{2 \varphi}{\sqrt{\pi} s \exp(\varphi^2)} \right. \\ \left. - \frac{2 \varphi}{\sqrt{\pi} s \exp\left[\left(\varphi + \frac{h s}{2 \varphi k_S}\right)^2\right]} \exp\left(\frac{h s}{k_S} + \frac{h^2 s^2}{4 \varphi^2 k_S^2}\right) \right\} + k_L \frac{2 \varphi n}{\sqrt{\pi} s} \cdot \frac{(T_P - T_F)}{\operatorname{erfc}(n \varphi)} \cdot \exp(-n^2 \varphi^2)$$

(98)

Rearranging the terms in a form for representing heat conduction parameters,

$$\varphi = \frac{C_{PS}(T_F - T_\infty)}{L \psi(s, \varphi)} \left\{ \frac{h s}{2 \varphi k_S} \exp\left(\frac{h s}{k_S} + \frac{h^2 s^2}{4 \varphi^2 k_S^2}\right) \operatorname{erfc}\left(\varphi + \frac{h s}{2 \varphi k_S}\right) + \frac{1}{\sqrt{\pi} \exp(\varphi^2)} \right. \\ \left. - \frac{1}{\sqrt{\pi} \exp\left[\left(\varphi + \frac{h s}{2 \varphi k_S}\right)^2\right]} \exp\left(\frac{h s}{k_S} + \frac{h^2 s^2}{4 \varphi^2 k_S^2}\right) \right\} \\ + \frac{C_{PL}(T_P - T_F)}{L} \frac{\alpha_L \rho_L}{\alpha_S \rho_S} \frac{n}{\sqrt{\pi} \operatorname{erfc}(n \varphi) \exp(n^2 \varphi^2)}$$

(99)

in which

$$N = \frac{\alpha_L \rho_L}{\alpha_S \rho_S} \quad (100)$$

By substituting the dimensionless numbers and heat transfer parameters,

$$\varphi = \frac{Ste_S}{\psi(s, \varphi)} \left\{ \frac{Biot}{2 \varphi} \exp\left(Biot + \frac{Biot^2}{4 \varphi^2}\right) \operatorname{erfc}\left(\varphi + \frac{Biot}{2 \varphi}\right) + \frac{1}{\sqrt{\pi} \exp(\varphi^2)} \right. \\ \left. - \frac{1}{\sqrt{\pi} \exp\left[\left(\varphi + \frac{Biot}{2 \varphi}\right)^2\right]} \exp\left(Biot + \frac{Biot^2}{4 \varphi^2}\right) \right\} + Ste_L N \frac{n}{\sqrt{\pi} \operatorname{erfc}(n \varphi) \exp(n^2 \varphi^2)}$$

(101)

where $Ste_L = \frac{C_{PL}(T_P - T_F)}{L}$ is the Stefan number considering the liquid phase.

Three-dimensional Two-Phase Moving Boundary Problem

The governing equations and the initial and boundary conditions for three-dimensional unsteady solidification are given by

$$\frac{\partial^2 T_S}{\partial x^2} + \frac{\partial^2 T_S}{\partial y^2} + \frac{\partial^2 T_S}{\partial z^2} = \frac{1}{\alpha_S} \frac{\partial T_S}{\partial t} \quad 0 < x < s_x(t), \quad 0 < y < s_y(t), \text{ and } 0 < z < s_z(t) \quad (102)$$

$$\frac{\partial^2 T_L}{\partial x^2} + \frac{\partial^2 T_L}{\partial y^2} + \frac{\partial^2 T_L}{\partial z^2} = \frac{1}{\alpha_L} \frac{\partial T_L}{\partial t} \quad s_x(t) < x < +\infty, s_y(t) < y < +\infty, \text{ and } s_z(t) < z < +\infty \quad (103)$$

$$t = 0, 0 < x < +\infty, T_L = T_{Px} \quad (104)$$

$$t = 0, 0 < y < +\infty, T_L = T_{Py} \quad (105)$$

$$t = 0, 0 < z < +\infty, T_L = T_{Pz} \quad (106)$$

$$t = 0, x = 0, h_x(T - T_{\infty_x}) = -k \frac{\partial T}{\partial x} \Big|_{x=-s_x} \quad (107)$$

$$t = 0, y = 0, h_y(T - T_{\infty_y}) = -k \frac{\partial T}{\partial y} \Big|_{y=-s_y} \quad (108)$$

$$t = 0, z = 0, h_z(T - T_{\infty_z}) = -k \frac{\partial T}{\partial z} \Big|_{z=-s_z} \quad (109)$$

$$t > 0, x = s(t), T_{S,L} = T_F \quad (110)$$

$$t > 0, y = s(t), T_{S,L} = T_F \quad (111)$$

$$t > 0, z = s(t), T_{S,L} = T_F \quad (112)$$

$$t > 0, x \rightarrow +\infty, T_L = T_{Px} \quad (113)$$

$$t > 0, y \rightarrow +\infty, T_L = T_{Py} \quad (114)$$

$$t > 0, z \rightarrow +\infty, T_L = T_{Pz} \quad (115)$$

$$\begin{aligned} \rho_S L \frac{ds}{dt} &= k_{S_x} \frac{\partial T_S}{\partial x} \Big|_{x=-s} + k_{S_y} \frac{\partial T_S}{\partial y} \Big|_{y=-s} + k_{S_z} \frac{\partial T_S}{\partial z} \Big|_{z=-s} \\ &- \left(k_{L_x} \frac{\partial T_L}{\partial x} \Big|_{x=+s} + k_{L_y} \frac{\partial T_L}{\partial y} \Big|_{y=+s} + k_{L_z} \frac{\partial T_L}{\partial z} \Big|_{z=+s} \right) \end{aligned} \quad (116)$$

where $\vec{s} = \hat{i}s_x + \hat{j}s_y + \hat{k}s_z$, $\vec{\rho}_S = \hat{i}\rho_{S_x} + \hat{j}\rho_{S_y} + \hat{k}\rho_{S_z}$, $\vec{k}_S = \hat{i}k_{S_x} + \hat{j}k_{S_y} + \hat{k}k_{S_z}$, $\vec{C}_{PS} = \hat{i}C_{PS_x} + \hat{j}C_{PS_y} + \hat{k}C_{PS_z}$, $\vec{\rho}_L = \hat{i}\rho_{L_x} + \hat{j}\rho_{L_y} + \hat{k}\rho_{L_z}$, $\vec{k}_L = \hat{i}k_{L_x} + \hat{j}k_{L_y} + \hat{k}k_{L_z}$ and $\vec{C}_{PL} = \hat{i}C_{PL_x} + \hat{j}C_{PL_y} + \hat{k}C_{PL_z}$. A three-dimensional solution for the temperature profile can be considered the product of the solutions in each x , y , and z axis, dimensional

$$t = t_x + t_y + t_z = \frac{s_x^2}{4\alpha_{S_x}\varphi^2} + \frac{s_y^2}{4\alpha_{S_y}\varphi^2} + \frac{s_z^2}{4\alpha_{S_z}\varphi^2} + \frac{2k_{S_x}s_x\varphi}{h_x\alpha_{S_x}} + \frac{2k_{S_y}s_y\varphi}{h_y\alpha_{S_y}} + \frac{2k_{S_z}s_z\varphi}{h_z\alpha_{S_z}} \quad (117a)$$

And dimensionless equation,

$$t^* = \frac{s_x^{*2}}{4Fo_x\varphi^2} + \frac{s_y^{*2}}{4Fo_y\varphi^2} + \frac{s_z^{*2}}{4Fo_z\varphi^2} + \frac{2s_x^*\varphi}{Biot_xFo_x} + \frac{2s_y^*\varphi}{Biot_yFo_y} + \frac{2s_z^*\varphi}{Biot_zFo_z} \quad (117b)$$

By substituting the similarity variable φ and setting $n_i = \sqrt{\frac{\alpha_{S_i}}{\alpha_{L_i}}}$,

$$\frac{\partial T_L}{\partial x} \Big|_{x=+s_x} = -\frac{2\varphi n_x}{\sqrt{\pi}s_x} \cdot \frac{(T_{Px}-T_F)}{\text{erfc}(n\varphi)} \cdot \exp(-n^2\varphi^2) \quad (118)$$

$$\frac{\partial T_L}{\partial y} \Big|_{y=+s_y} = -\frac{2\varphi n_y}{\sqrt{\pi}s_y} \cdot \frac{(T_{Py}-T_F)}{\text{erfc}(n\varphi)} \cdot \exp(-n^2\varphi^2) \quad (119)$$

$$\frac{\partial T_L}{\partial z} \Big|_{z=+s_z} = -\frac{2\varphi n_z}{\sqrt{\pi}s_z} \cdot \frac{(T_{Pz}-T_F)}{\text{erfc}(n\varphi)} \cdot \exp(-n^2\varphi^2) \quad (120)$$

and, by writing s in relation to the similarity variables,

$$2\sqrt{\alpha_{S_i}t} = \frac{s_i}{\varphi} \quad (121)$$

$$\frac{T_{Lx}(x,s_x)-T_{Px}}{T_F-T_{Px}} = \theta_{Lx} = \frac{1}{1-\text{erf}(n\varphi)} \cdot \left[1 - \text{erf}\left(n_x\varphi \frac{x}{s_x}\right) \right] \quad (122)$$

$$\frac{T_{Ly}(y, s_y) - T_{Py}}{T_F - T_{Py}} = \theta_{Ly} = \frac{1}{1 - \text{erf}(n\varphi)} \cdot \left[1 - \text{erf}\left(n\varphi \frac{y}{s_y}\right) \right] \quad (123)$$

$$\frac{T_{Lz}(z, s_z) - T_{Pz}}{T_F - T_{Pz}} = \theta_{Lz} = \frac{1}{1 - \text{erf}(n\varphi)} \cdot \left[1 - \text{erf}\left(n\varphi \frac{z}{s_z}\right) \right] \quad (124)$$

The three-dimensional solution for the temperature profile in the liquid phase can be expressed as follows:

$$\theta_L(x, y, z, s_x, s_y, s_z) = \theta_{Lx}(x, s_x) \theta_{Ly}(y, s_y) \theta_{Lz}(z, s_z) \quad (125)$$

that is,

$$\begin{aligned} \theta_L(x, y, z, s_x, s_y, s_z) &= \theta_{Lx}(x, s_x) \theta_{Ly}(y, s_y) \theta_{Lz}(z, s_z) = \left[\frac{T_L(x, y, z, s_x, s_y, s_z) - T_{Pi}}{T_F - T_{Pi}} \right] \\ &= \left[\frac{T_{Sx}(x, s_x) - T_F}{T_F - T_{Px}} \right] \left[\frac{T_{Sy}(y, s_y) - T_F}{T_F - T_{Py}} \right] \left[\frac{T_{Sz}(z, s_z) - T_F}{T_F - T_{Pz}} \right] \\ &= \left\{ \frac{1}{1 - \text{erf}(n\varphi)} \cdot \left[1 - \text{erf}\left(n\varphi \frac{x}{s_x}\right) \right] \right\} \left\{ \frac{1}{1 - \text{erf}(n\varphi)} \cdot \left[1 - \text{erf}\left(n\varphi \frac{y}{s_y}\right) \right] \right\} \left\{ \frac{1}{1 - \text{erf}(n\varphi)} \cdot \left[1 - \text{erf}\left(n\varphi \frac{z}{s_z}\right) \right] \right\} \end{aligned} \quad (126)$$

By applying the temperature gradients in the solid and liquid phases in $\nabla T_S|_{X=-s}$ and $\nabla T_L|_{X=+s}$,

$$\rho_S L \frac{ds}{dt} = (k_S \nabla T_S)|_{X=-s} - (k_L \nabla T_L)|_{X=+s} \quad (127)$$

$$\frac{ds}{dt} = \frac{2\varphi^2 \alpha_S}{s} \quad (128)$$

in which $s = \sqrt{s_x^2 + s_y^2 + s_z^2}$

$$\begin{aligned}
\rho_S L \frac{2\varphi^2 \alpha_S}{s} = & k_{S_x} \frac{(T_F - T_{\infty_x})}{\psi(s_x, \varphi)} \left\{ \frac{h_x}{k_{S_x}} \exp\left(\frac{h_x s_x}{k_{S_x}} + \frac{h_x^2 s_x^2}{4 \varphi^2 k_{S_x}^2}\right) \operatorname{erfc}\left(\varphi + \frac{h_x s_x}{2 \varphi k_{S_x}}\right) + \frac{2\varphi}{\sqrt{\pi} s_x \exp(\varphi^2)} \right. \\
& - \frac{2\varphi}{\sqrt{\pi} s_x \exp\left[\left(\varphi + \frac{h_x s_x}{2 \varphi k_{S_x}}\right)^2\right]} \exp\left(\frac{h_x s_x}{k_{S_x}} + \frac{h_x^2 s_x^2}{4 \varphi^2 k_{S_x}^2}\right) \left. \right\} \\
& + k_{S_y} \frac{(T_F - T_{\infty_y})}{\psi(s_y, \varphi)} \left\{ \frac{h_y}{k_{S_y}} \exp\left(\frac{h_y s_y}{k_{S_y}} + \frac{h_y^2 s_y^2}{4 \varphi^2 k_{S_y}^2}\right) \operatorname{erfc}\left(\varphi + \frac{h_y s_y}{2 \varphi k_{S_y}}\right) + \frac{2\varphi}{\sqrt{\pi} s_y \exp(\varphi^2)} \right. \\
& - \frac{2\varphi}{\sqrt{\pi} s_y \exp\left[\left(\varphi + \frac{h_y s_y}{2 \varphi k_{S_y}}\right)^2\right]} \exp\left(\frac{h_y s_y}{k_{S_y}} + \frac{h_y^2 s_y^2}{4 \varphi^2 k_{S_y}^2}\right) \left. \right\} \\
& + k_{S_z} \frac{(T_F - T_{\infty_z})}{\psi(s_z, \varphi)} \left\{ \frac{h_z}{k_{S_z}} \exp\left(\frac{h_z s_z}{k_{S_z}} + \frac{h_z^2 s_z^2}{4 \varphi^2 k_{S_z}^2}\right) \operatorname{erfc}\left(\varphi + \frac{h_z s_z}{2 \varphi k_{S_z}}\right) + \frac{2\varphi}{\sqrt{\pi} s_z \exp(\varphi^2)} \right. \\
& - \frac{2\varphi}{\sqrt{\pi} s_z \exp\left[\left(\varphi + \frac{h_z s_z}{2 \varphi k_{S_z}}\right)^2\right]} \exp\left(\frac{h_z s_z}{k_{S_z}} + \frac{h_z^2 s_z^2}{4 \varphi^2 k_{S_z}^2}\right) \left. \right\} + k_{L_x} \frac{2\varphi n_x}{\sqrt{\pi} s_x} \cdot \frac{(T_{P_x} - T_F)}{\operatorname{erfc}(n_x \varphi)} \\
& \cdot \exp(-n_x^2 \varphi^2) + k_{L_y} \frac{2\varphi n_y}{\sqrt{\pi} s_y} \cdot \frac{(T_{P_y} - T_F)}{\operatorname{erfc}(n_y \varphi)} \cdot \exp(-n_y^2 \varphi^2) + k_{L_z} \frac{2\varphi n_z}{\sqrt{\pi} s_z} \cdot \frac{(T_{P_z} - T_F)}{\operatorname{erfc}(n_z \varphi)} \\
& \cdot \exp(-n_z^2 \varphi^2)
\end{aligned}
\tag{129}$$

By arranging Eq. (130) so that it can represent a set of meaningful heat transfer parameters,

$$\begin{aligned}
\varphi = & \frac{C_{PS_x}(T_F - T_{\infty_x})}{L_x \psi(s_x, \varphi)} \left\{ \frac{h_x s_x}{2\varphi k_{S_x}} \exp\left(\frac{h_x s_x}{k_{S_x}} + \frac{h_x^2 s_x^2}{4\varphi^2 k_{S_x}^2}\right) \operatorname{erfc}\left(\varphi + \frac{h_x s_x}{2\varphi k_{S_x}}\right) + \frac{1}{\sqrt{\pi} \exp(\varphi^2)} \right. \\
& - \frac{1}{\sqrt{\pi} \exp\left[\left(\varphi + \frac{h_x s_x}{2\varphi k_{S_x}}\right)^2\right]} \exp\left(\frac{h_x s_x}{k_{S_x}} + \frac{h_x^2 s_x^2}{4\varphi^2 k_{S_x}^2}\right) \left. \right\} \\
& + \frac{C_{PS_y}(T_F - T_{\infty_y})}{L_y \psi(s_y, \varphi)} \left\{ \frac{h_y s_y}{2\varphi k_{S_y}} \exp\left(\frac{h_y s_y}{k_{S_y}} + \frac{h_y^2 s_y^2}{4\varphi^2 k_{S_y}^2}\right) \operatorname{erfc}\left(\varphi + \frac{h_y s_y}{2\varphi k_{S_y}}\right) + \frac{1}{\sqrt{\pi} \exp(\varphi^2)} \right. \\
& - \frac{1}{\sqrt{\pi} \exp\left[\left(\varphi + \frac{h_y s_y}{2\varphi k_{S_y}}\right)^2\right]} \exp\left(\frac{h_y s_y}{k_{S_y}} + \frac{h_y^2 s_y^2}{4\varphi^2 k_{S_y}^2}\right) \left. \right\} \\
& + \frac{C_{PS_z}(T_F - T_{\infty_z})}{L_z \psi(s_z, \varphi)} \left\{ \frac{h_z s_z}{2\varphi k_{S_z}} \exp\left(\frac{h_z s_z}{k_{S_z}} + \frac{h_z^2 s_z^2}{4\varphi^2 k_{S_z}^2}\right) \operatorname{erfc}\left(\varphi + \frac{h_z s_z}{2\varphi k_{S_z}}\right) + \frac{1}{\sqrt{\pi} \exp(\varphi^2)} \right. \\
& - \frac{1}{\sqrt{\pi} \exp\left[\left(\varphi + \frac{h_z s_z}{2\varphi k_{S_z}}\right)^2\right]} \exp\left(\frac{h_z s_z}{k_{S_z}} + \frac{h_z^2 s_z^2}{4\varphi^2 k_{S_z}^2}\right) \left. \right\} \\
& + \frac{C_{PL_x}(T_{P_x} - T_F)}{L_x} \frac{\alpha_{L_x} \rho_{L_x}}{\alpha_{S_x} \rho_{S_x}} \frac{n_x}{\sqrt{\pi} \operatorname{erfc}(n_x \varphi) \exp(n_x^2 \varphi^2)} \\
& + \frac{C_{PL_y}(T_{P_y} - T_F)}{L_y} \frac{\alpha_{L_y} \rho_{L_y}}{\alpha_{S_y} \rho_{S_y}} \frac{n_y}{\sqrt{\pi} \operatorname{erfc}(n_y \varphi) \exp(n_y^2 \varphi^2)} \\
& + \frac{C_{PL_z}(T_{P_z} - T_F)}{L_z} \frac{\alpha_{L_z} \rho_{L_z}}{\alpha_{S_z} \rho_{S_z}} \frac{n_z}{\sqrt{\pi} \operatorname{erfc}(n_z \varphi) \exp(n_z^2 \varphi^2)}
\end{aligned}
\tag{130}$$

Eq. (130) can be expressed according to dimensionless numbers

$$\begin{aligned}
\varphi = & \frac{Ste_x}{\psi(Biot_x, \varphi)} \left\{ \frac{Biot_x}{2\varphi} \exp\left(Biot_x + \frac{Biot_x^2}{4\varphi^2}\right) \operatorname{erfc}\left(\varphi + \frac{Biot_x}{2\varphi}\right) + \frac{1}{\sqrt{\pi} \exp(\varphi^2)} \right. \\
& - \frac{1}{\sqrt{\pi} \exp\left[\left(\varphi + \frac{Biot_x}{2\varphi}\right)^2\right]} \exp\left(Biot_x + \frac{Biot_x^2}{4\varphi^2}\right) \left. \right\} \\
& + \frac{Ste_y}{\psi(Biot_y, \varphi)} \left\{ \frac{Biot_y}{2\varphi} \exp\left(Biot_y + \frac{Biot_y^2}{4\varphi^2}\right) \operatorname{erfc}\left(\varphi + \frac{Biot_y}{2\varphi}\right) + \frac{1}{\sqrt{\pi} \exp(\varphi^2)} \right. \\
& - \frac{1}{\sqrt{\pi} \exp\left[\left(\varphi + \frac{Biot_y}{2\varphi}\right)^2\right]} \exp\left(Biot_y + \frac{Biot_y^2}{4\varphi^2}\right) \left. \right\} \\
& + \frac{Ste_z}{\psi(Biot_z, \varphi)} \left\{ \frac{Biot_z}{2\varphi} \exp\left(Biot_z + \frac{Biot_z^2}{4\varphi^2}\right) \operatorname{erfc}\left(\varphi + \frac{Biot_z}{2\varphi}\right) + \frac{1}{\sqrt{\pi} \exp(\varphi^2)} \right. \\
& - \frac{1}{\sqrt{\pi} \exp\left[\left(\varphi + \frac{Biot_z}{2\varphi}\right)^2\right]} \exp\left(Biot_z + \frac{Biot_z^2}{4\varphi^2}\right) \left. \right\} + Ste_{Lx} N_x \frac{n_x}{\sqrt{\pi} \operatorname{erfc}(n_x \varphi) \exp(n_x^2 \varphi^2)} \\
& + Ste_{Ly} N_y \frac{n_y}{\sqrt{\pi} \operatorname{erfc}(n_y \varphi) \exp(n_y^2 \varphi^2)} + Ste_{Lz} N_z \frac{n_z}{\sqrt{\pi} \operatorname{erfc}(n_z \varphi) \exp(n_z^2 \varphi^2)}
\end{aligned}
\tag{131}$$

where $Ste_{L_i} = \frac{C_{PL_i}(T_{P_i} - T_F)}{L_i}$ is the Stefan number considering the liquid phase and $N_i = \frac{\alpha_{L_i} \rho_{L_i}}{\alpha_{S_i} \rho_{S_i}}$ represent the ratio between the product of thermal diffusivity and the density of the liquid and solid phases, respectively.

Considerations for Calculating Interface Velocity and Position

The current solution is considerably complex when formulating simple equations for the solid-liquid interface velocity. By writing $t = \gamma s^2 + \delta s$, deriving and rearranging it as $\frac{ds}{dt} = v = \frac{1}{2\gamma s + \delta}$ [63]. The value of $\gamma = \frac{1}{4\alpha_S \varphi^2}$ is straightforward. However, determining δ requires a different approach: $\frac{dt}{ds} = 2\gamma s + \delta = \frac{1}{v}$, so $\delta = \frac{1}{v} - 2\gamma s$. Finally, expressing the velocity v in terms of the thermal gradients of the solid and liquid phases provides

$$\frac{ds(t)}{dt} = v = \frac{1}{\rho_S L} (k_S \cdot \nabla T_S|_{\chi=-s} - k_L \cdot \nabla T_L|_{\chi=+s})
\tag{132}$$

The value of δ can now be determined as,

$$\delta = \frac{\rho_S L}{k_S \cdot \nabla T_S|_{\chi=-s} - k_L \cdot \nabla T_L|_{\chi=+s}} - 2\gamma s
\tag{133}$$

for solidification time,

$$t = \gamma s^2 + \delta s
\tag{134}$$

and velocity,

$$v = \frac{1}{2\gamma s + \delta}
\tag{135}$$

The thermal gradients of the liquid (∇T_L) and solid (∇T_S) phases are analytical expressions derived in this work. Here, k represents the thermal conductivity, expressed as $k = \hat{i}k_x + \hat{j}k_y + \hat{k}k_z$, and χ is the positional vector defined by $\chi = \hat{i}x + \hat{j}y + \hat{k}z$. Equation (132) is complex and too lengthy to present fully here, but it remains an analytical equation.

III. Results And Discussion

The analytical solutions formulated in this investigation will undergo analysis based on the following criteria: one-dimensional one-phase and two-phase, as well as three-dimensional one-phase and two-phase. Furthermore, Table 1 provides data on the thermodynamic properties of pure Al in its solid and liquid phases.

Table 1 Thermophysical properties of pure Al.						
Properties	Symbol	Units	Al	Al33.2wt%Cu	Sn39wt%Pb	Water at 5000 m
Temperature of fusion	T_F	K	933.15	821.15	456	271.15
Thermal conductivity (solid)	k_S	$W m^{-1} K^{-1}$	220	155	54.7	2.38
Thermal conductivity (liquid)	k_L	$W m^{-1} K^{-1}$	91	71	31.7	0.6577
Density (solid)	ρ_s	$kg m^{-3}$	2550	3410	8840	919.76
Density (liquid)	ρ_l	$kg m^{-3}$	2368	3240	8400	969.89
Specific heat (solid)	c_s	$J kg^{-1} K^{-1}$	1181	1070	186.2	1950
Specific heat (liquid)	c_L	$J kg^{-1} K^{-1}$	1086	895	212.9	4192.94
Latent heat of fusion	ΔH	$J kg^{-1}$	397500	350000	47560	341620

The analytical calculations are plotted against the numerical results for one-phase transient solidification considering the solid/liquid interface position versus time and temperature profile, according to Figure 3A and Figure 3B, respectively. The global heat transfer coefficients h_G are constant and equal to 500, 1000, 3000, 7000 and 18000 $W m^{-1} K^{-1}$. The numerical method [28,60,61] cannot be carried out in this study as published. Based on the present proposition: Firstly, the second order Biot number, $Biot = \frac{h^2 at}{k^2}$, concerning the thermal diffusion layer resistance is absent. Secondly, the numerical model has a function called $dgdT$, which relates the dependence of the liquid volume fraction on temperature associated with an equation governing the latent heat release rule in the energy equation in terms of solute concentration density field. For pure materials, this is not the case. Consequently, this numerical solution scheme fails to accurately predict the solidification of pure materials, by adding an artificial amount of latent heat which dislocates the global heat transfer coefficient. The corresponding numerical solution of the energy equation for pure and eutectic materials under convective boundary condition, associated with the other transport equations is being studied to develop a suitable solver to this problem and will be discussed in a forthcoming publication.

In Figure 4, a two-phase analytical solution is applied for the interface position as a function of melt superheat for 0.1, 5, 35, 55, and 105K. When the same Biot number and melt superheat are considered for all the superheating events, the interface position as a function of time is not sensitive. However, the same cannot be said for the velocity of the solid/liquid interface, as shown in Fig. 5, for which the speed is $\sim 14 \text{ mm s}^{-1}$ for the given combination of both the highest Biot and superheat. It is well known that under transient experimental solidification conditions, the Biot number usually depends on overheating and cannot be kept constant.

Figures 6 and 7 represent the thermal gradients for the liquid and solid phases, respectively, in the vicinity of the solid/liquid interface against position. The melt superheat is more sensitive to the thermal gradient of the liquid and less sensitive to the gradient of the solid for a given Biot and melt superheat.

The temperature profile was calculated as a function of both the Biot number and melt superheat, as shown in Fig. 8. The temperature at $x = 0$ depends only on the Biot number for a given Biot and melt superheat. However, the temperature profile of the solid phase is affected.

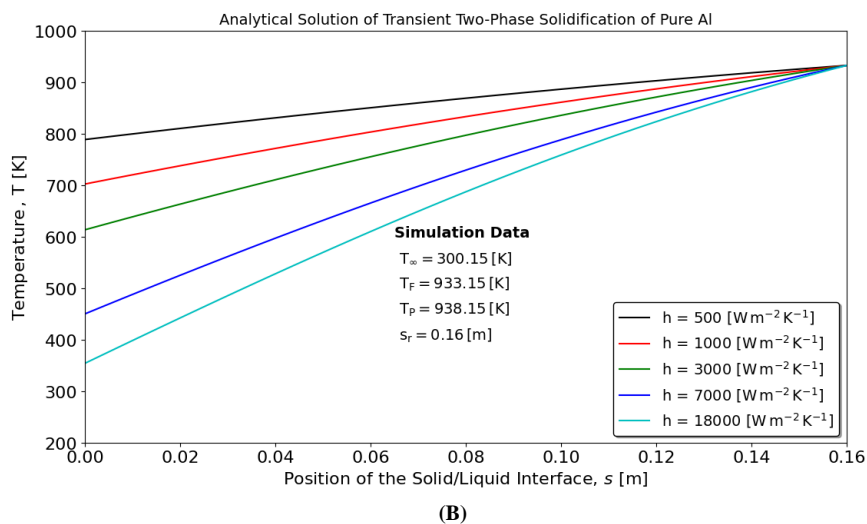
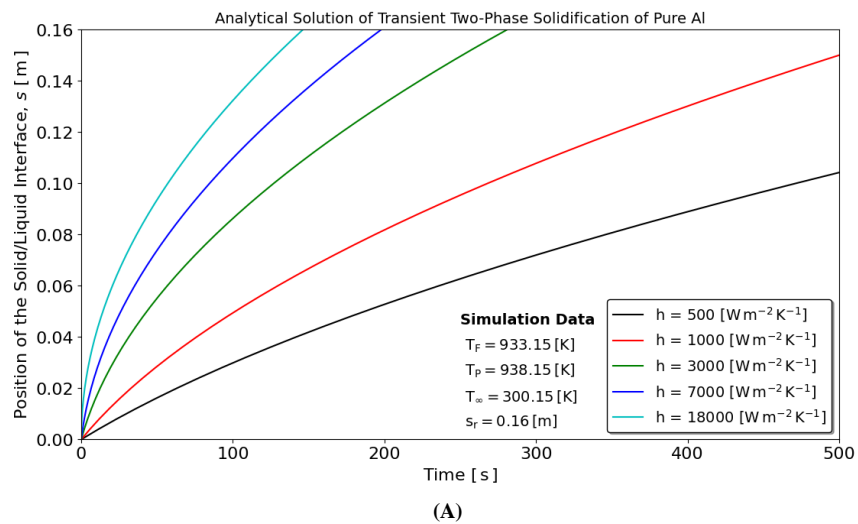
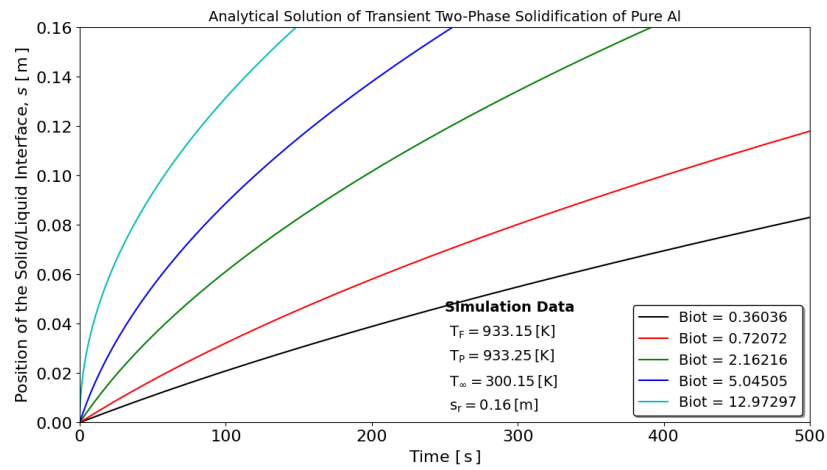
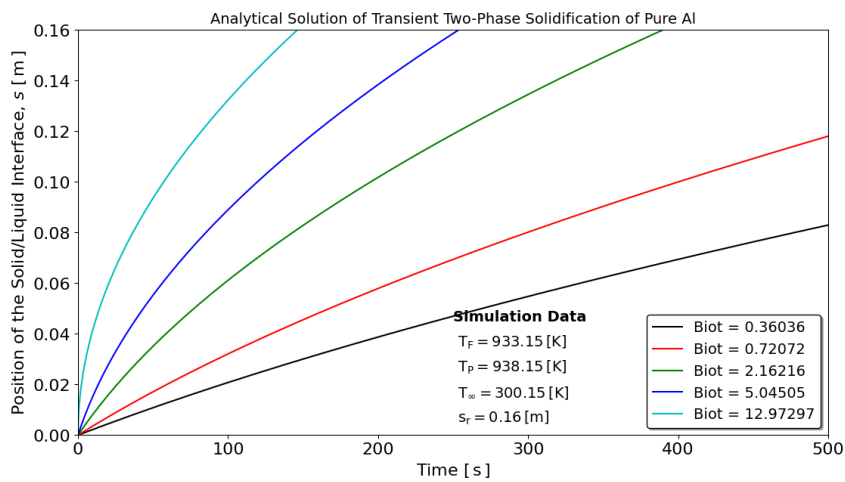


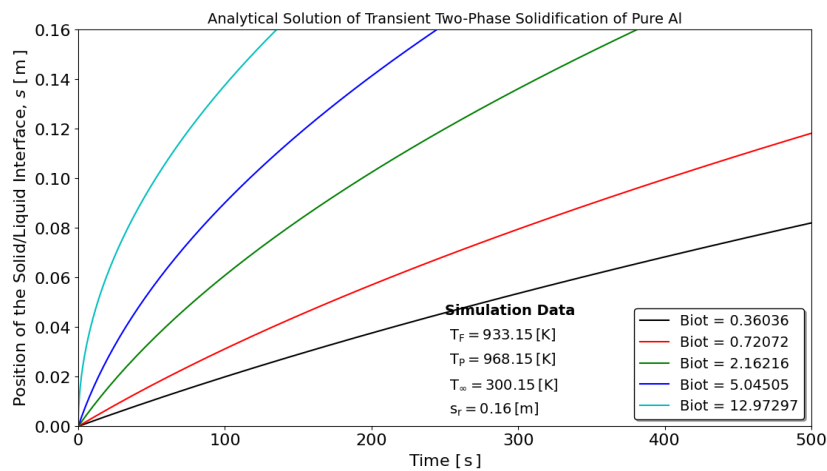
Figure 3 Analytical solution of unidimensional one-phase solidification against numerical simulation: (A) Position of solid/liquid interface as a function of time, and (B) Temperature profiles.



(A)



(B)



(C)

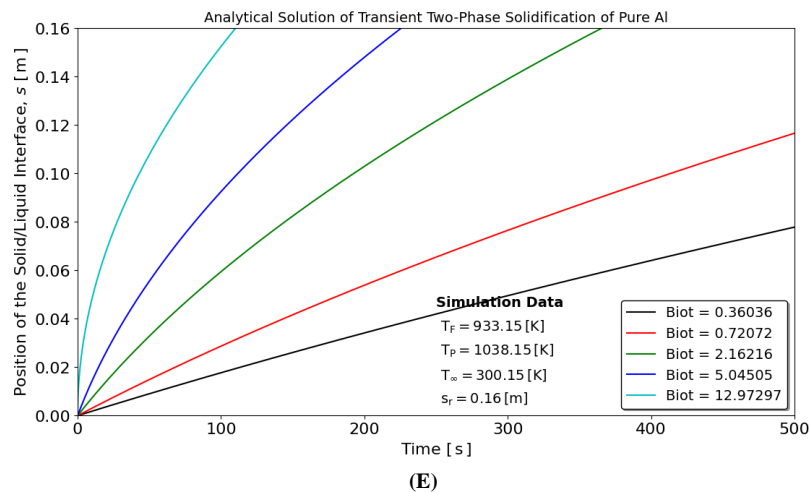
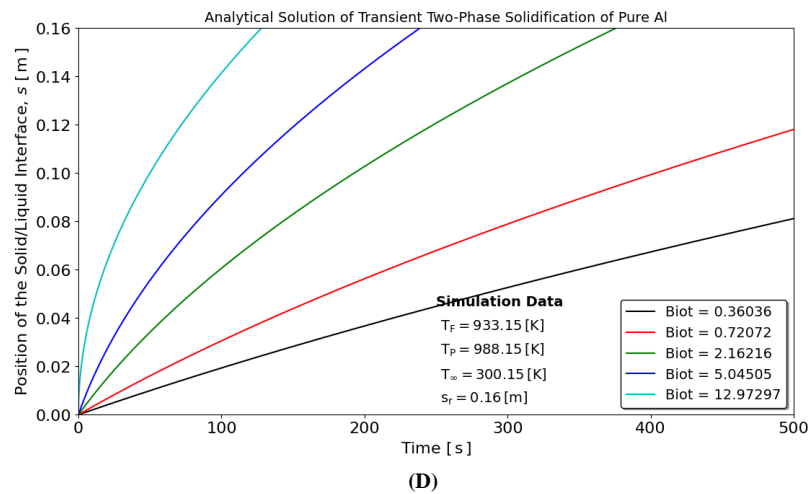
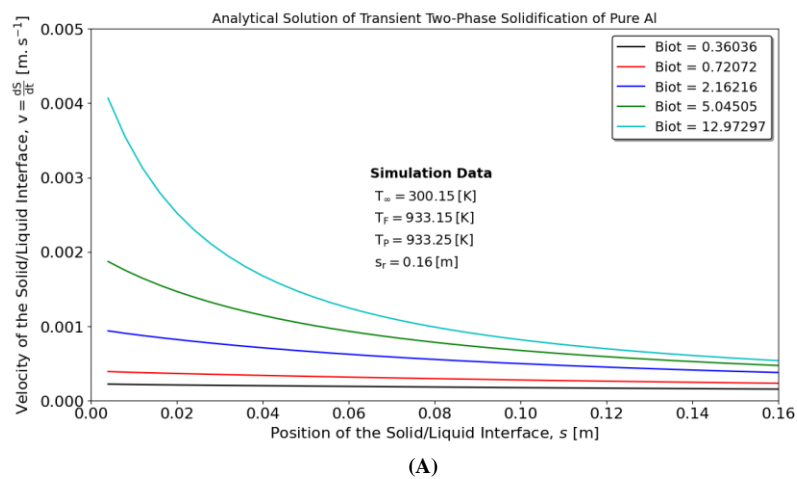
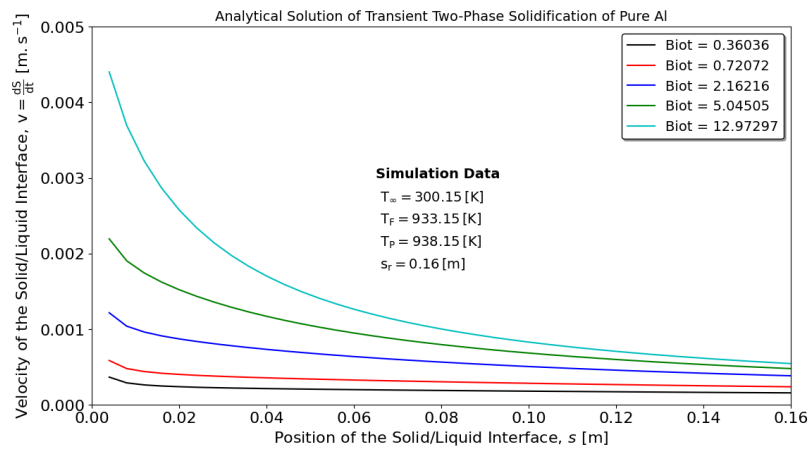
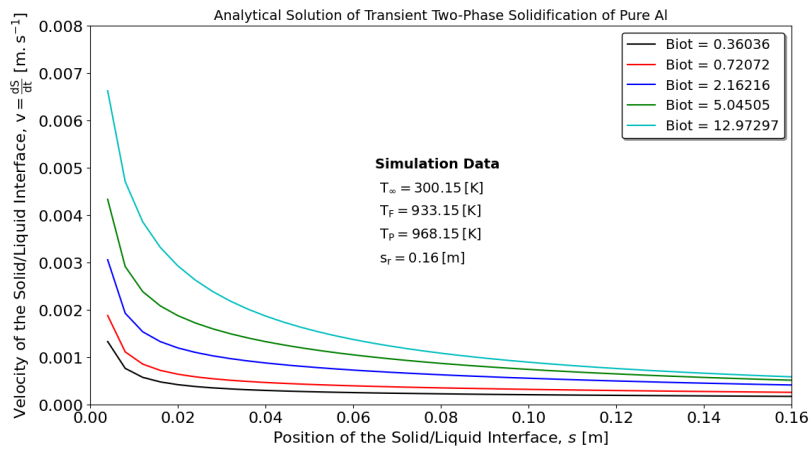


Figure 4 Analytical solution for one-dimensional two-phase solidification for interface position as a function of melt superheat: (A) 0.1K, (B) 5K, (C) 35K, (D) 55K, and (E) 105K.

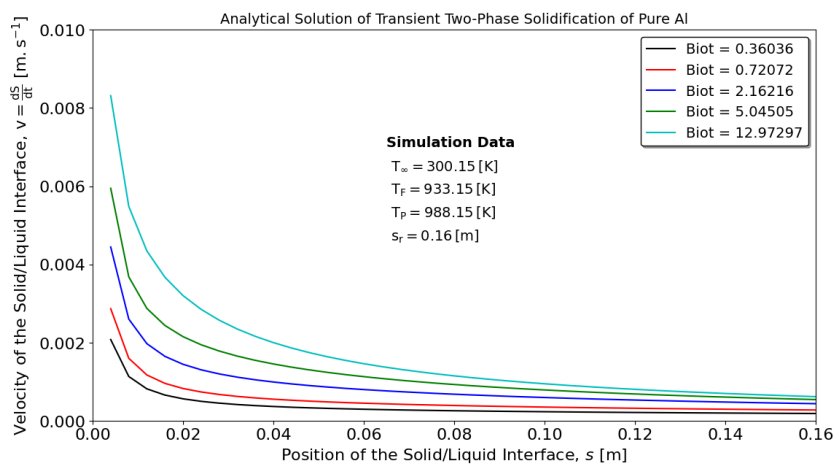




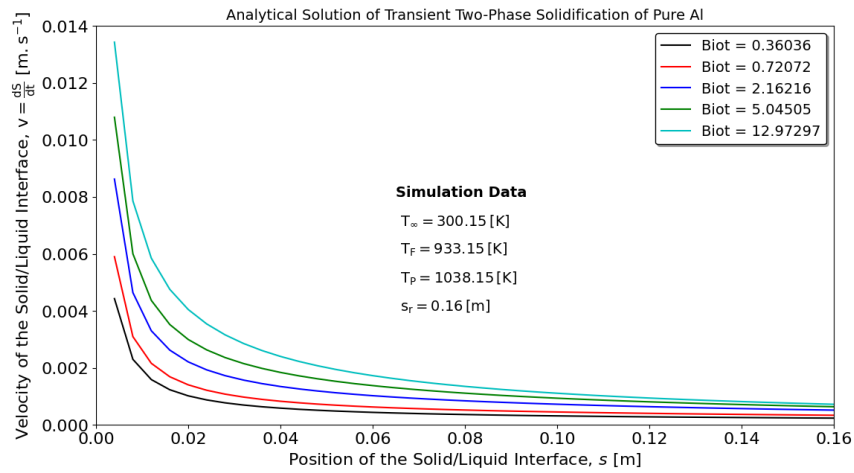
(B)



(C)

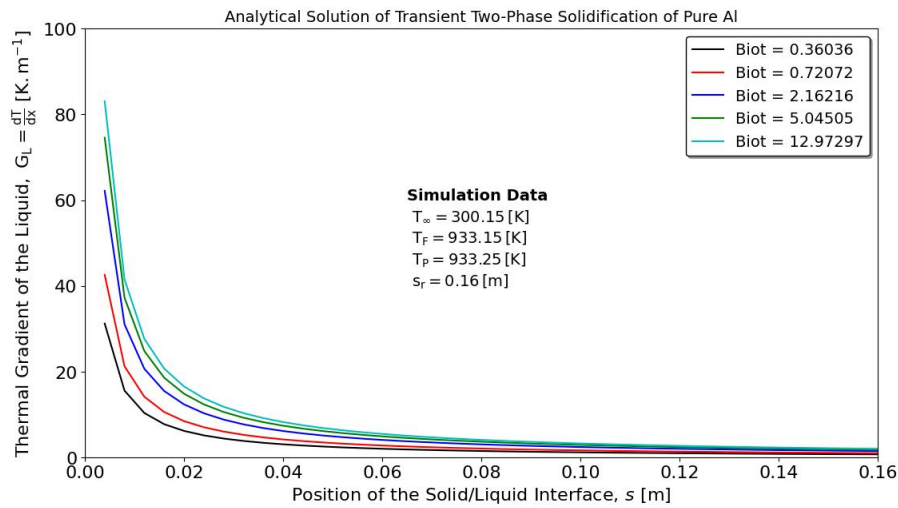


(D)

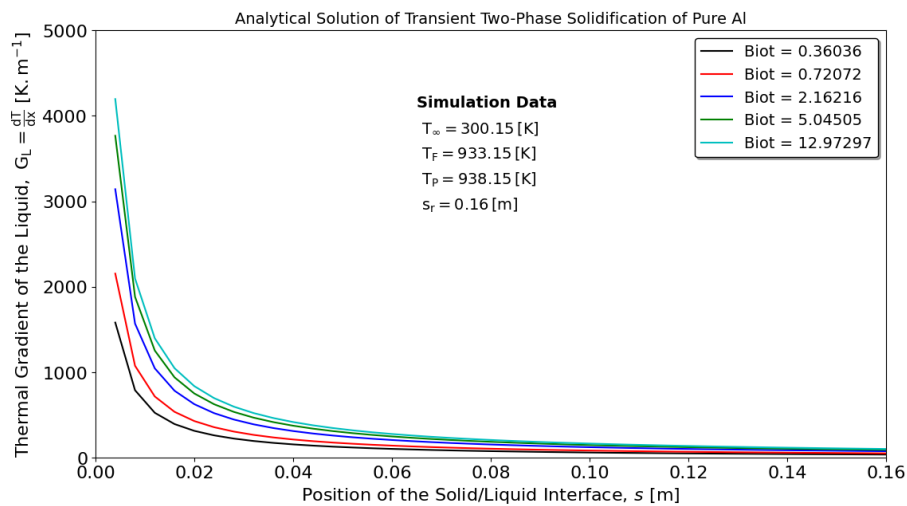


(E)

Figure 5 Analytical solution for one-dimensional two-phase solidification for interface velocity as a function of melt superheat: (A) 0.1K, (B) 5K, (C) 35K, (D) 55K, and (E) 105K.



(A)



(B)

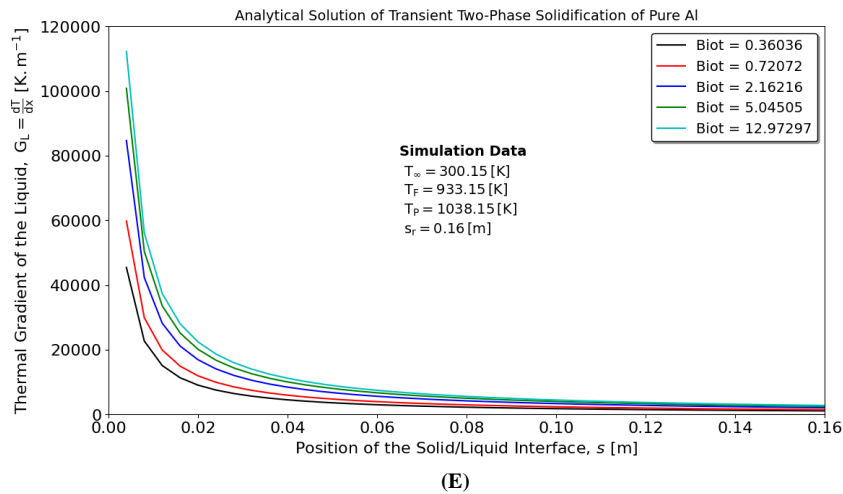
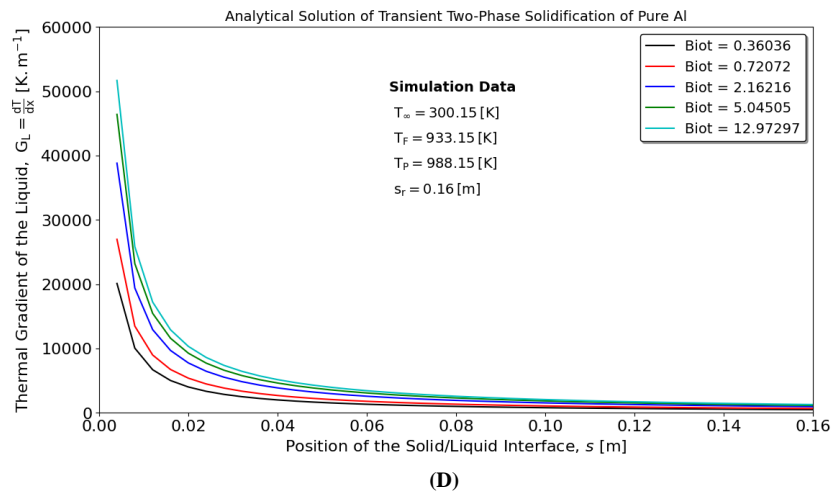
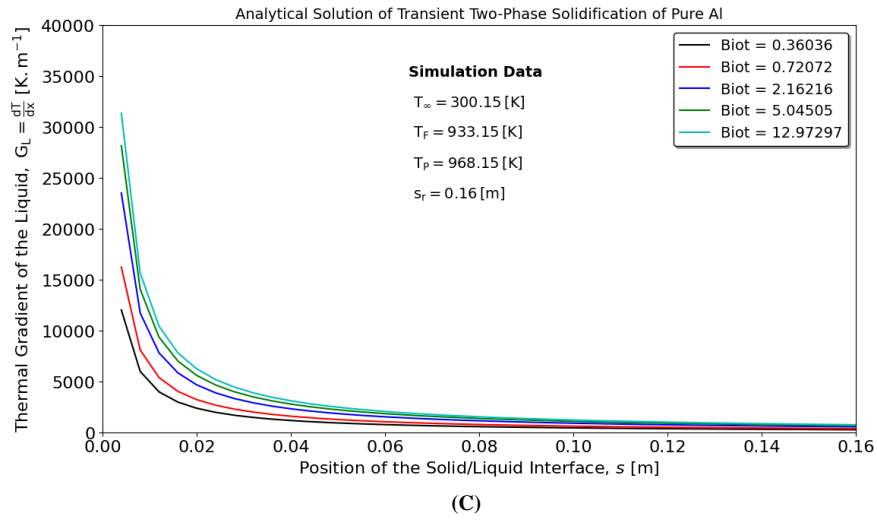
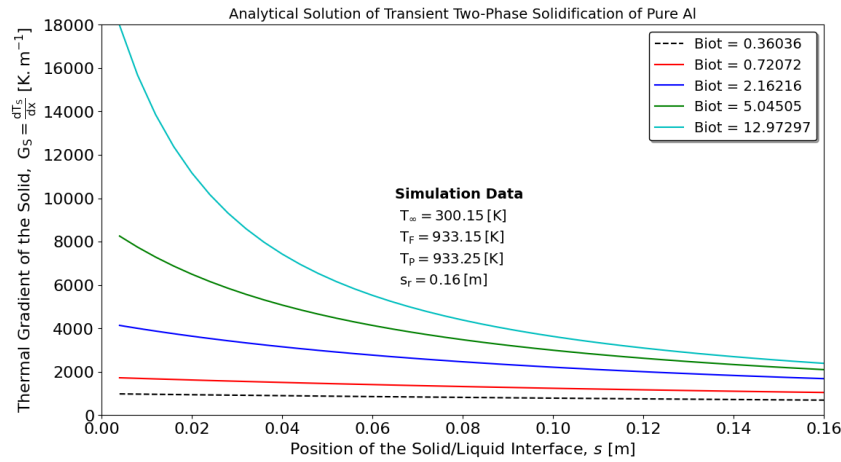
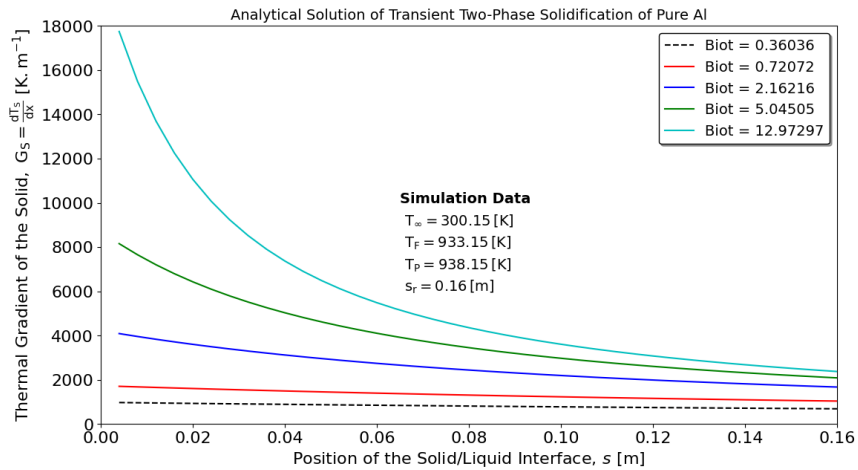


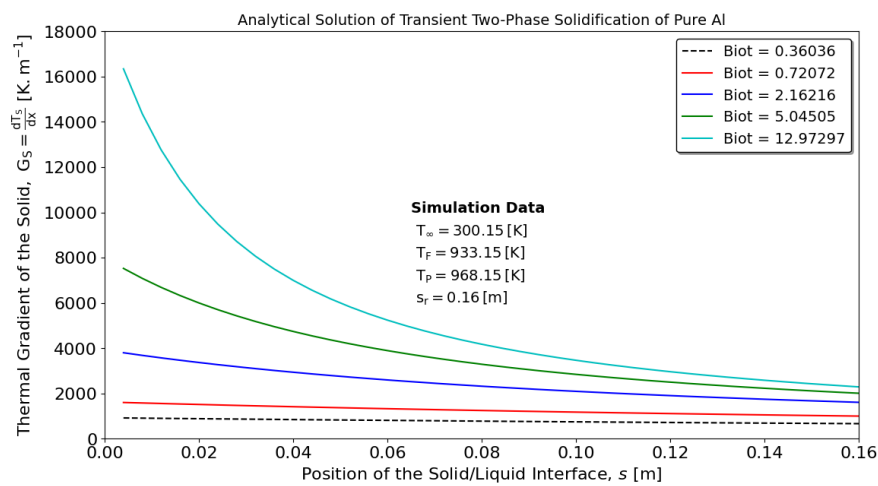
Figure 6 Analytical solution for one-dimensional two-phase solidification for thermal gradient of the liquid as a function of melt superheat: (A) 0.1K, (B) 5K, (C) 35K, (D) 55K, and (E) 105K



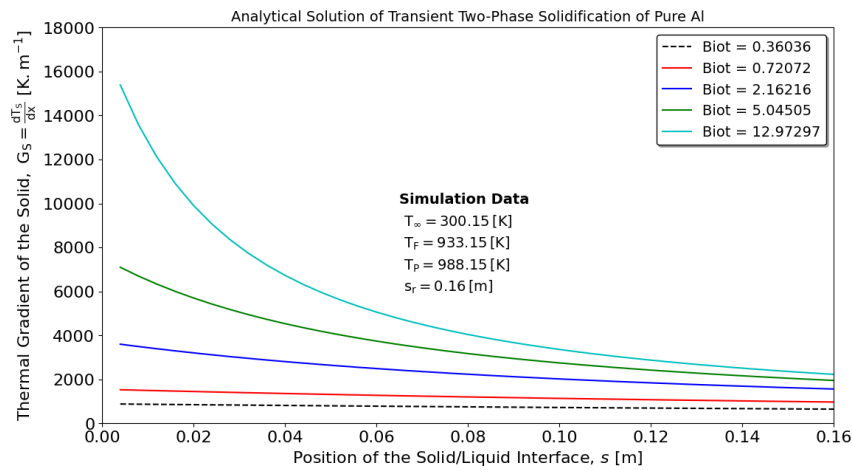
(A)



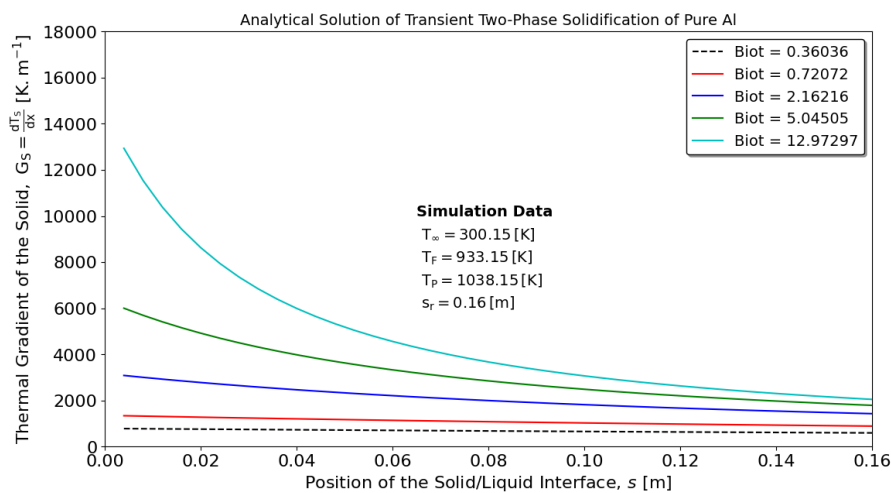
(B)



(C)

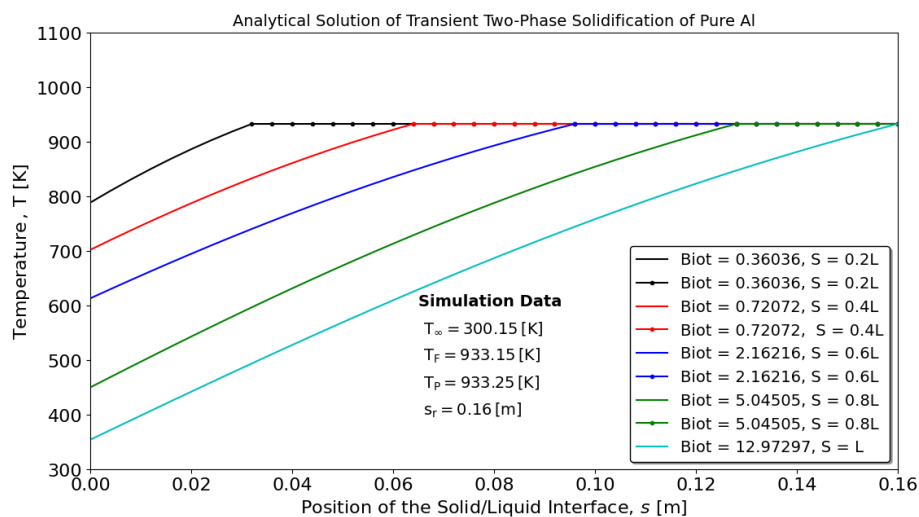


(D)

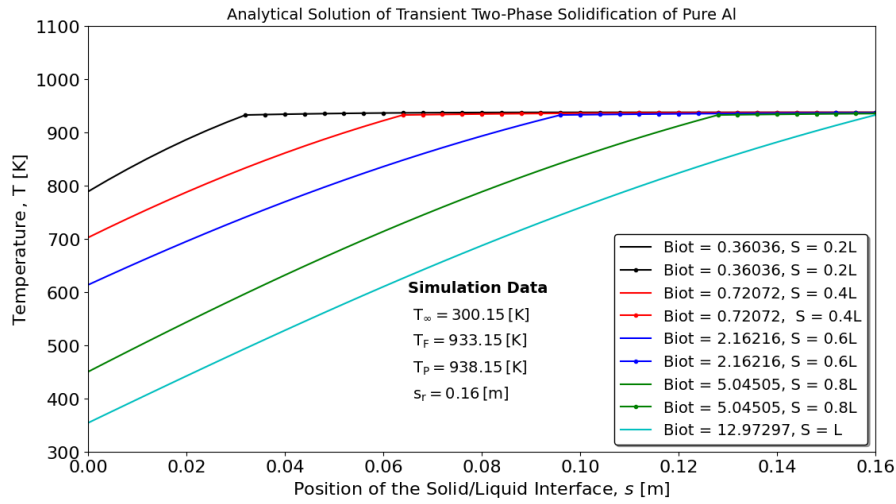


(E)

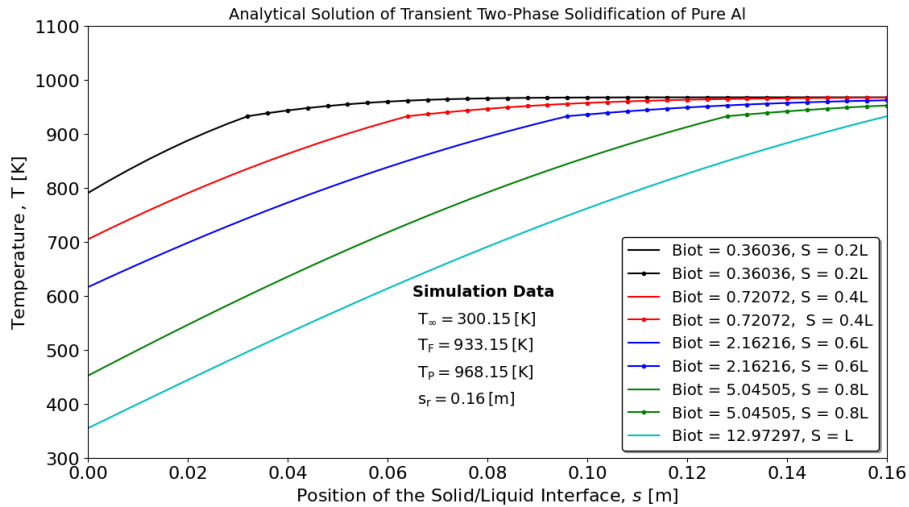
Figure 7 Analytical solution for one-dimensional two-phase solidification for thermal gradient of the solid as a function of melt superheat: (A) 5K, (B) 35K, (C) 55K, and (D) 105K.



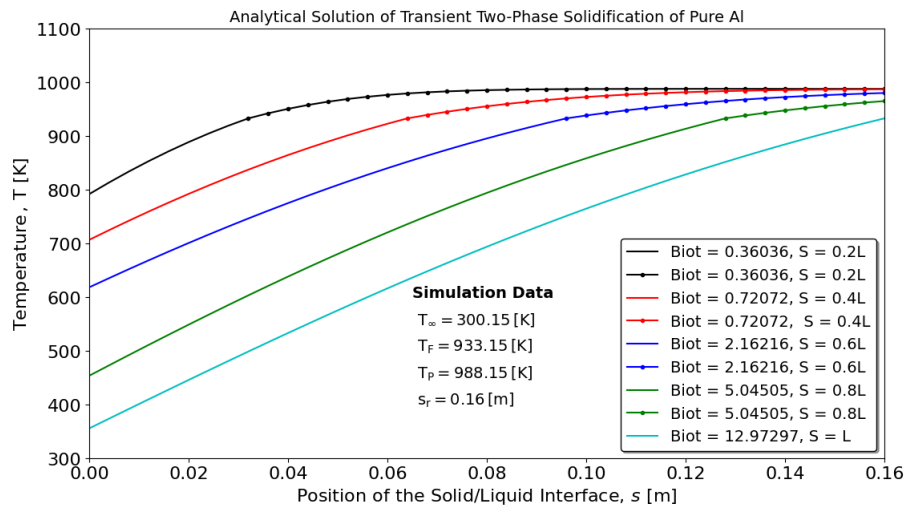
(A)



(B)



(C)



(D)

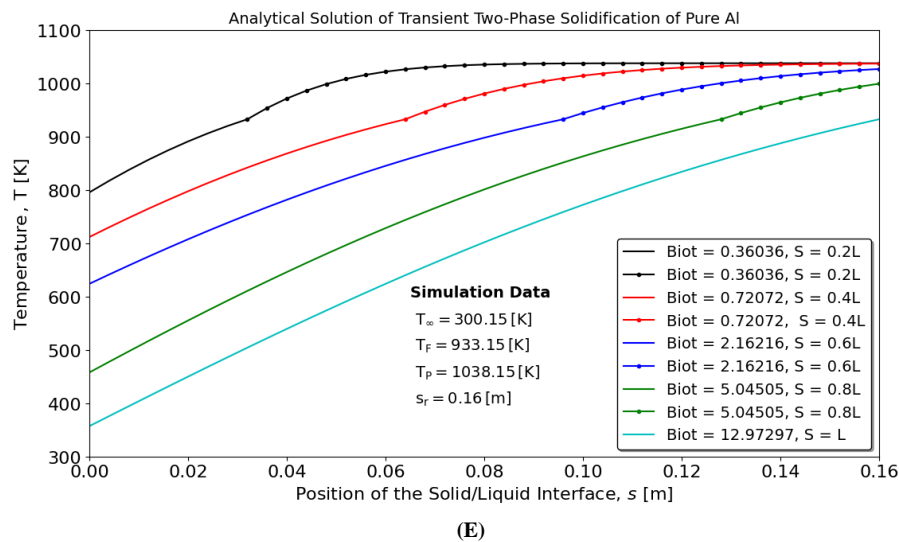
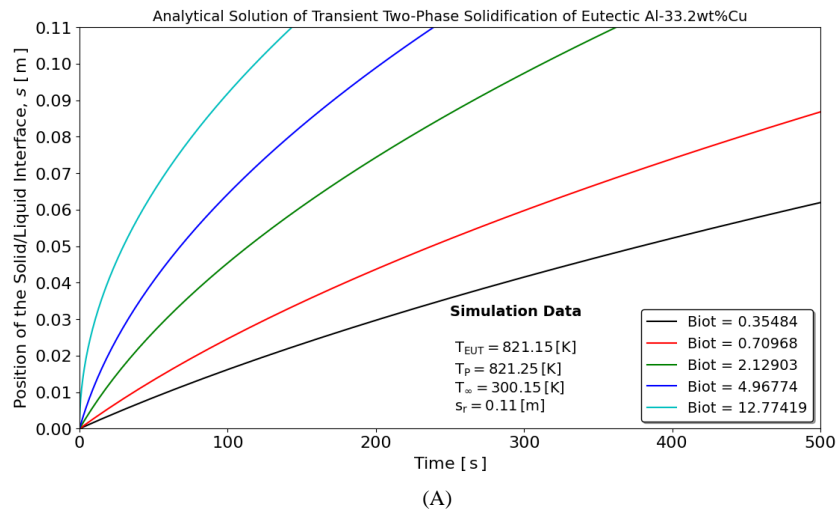
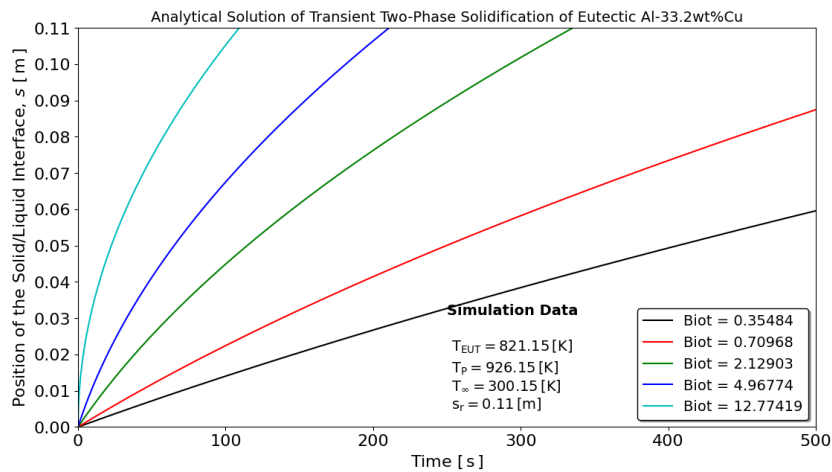


Figure 8 Analytical solution for one-dimensional two-phase solidification for temperature profile as a function of melt superheat: (A) 0.1K, (B) 5K, (C) 35K, (D) 55K, and (E) 105K.

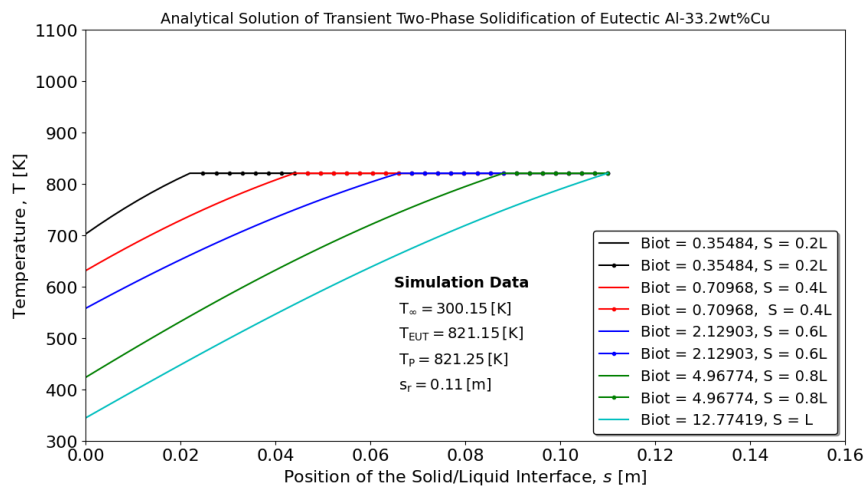
The temperature profile was calculated as a function of the Biot number and melt superheat, as shown in Fig. 8. The temperature at $x = 0$ depends only on the Biot number for a given Biot and melt superheat. However, the temperature profile of the solid phase is affected.

Figure 9 compares the position of the solid/liquid interface as a function of time, temperature profiles, and thermal gradients of the liquid phase for eutectic Al33.2wt%Cu in terms of Biot and melt superheat of 0.1K and 105K. The thermal gradient of the liquid phase increases rapidly with melt superheat.

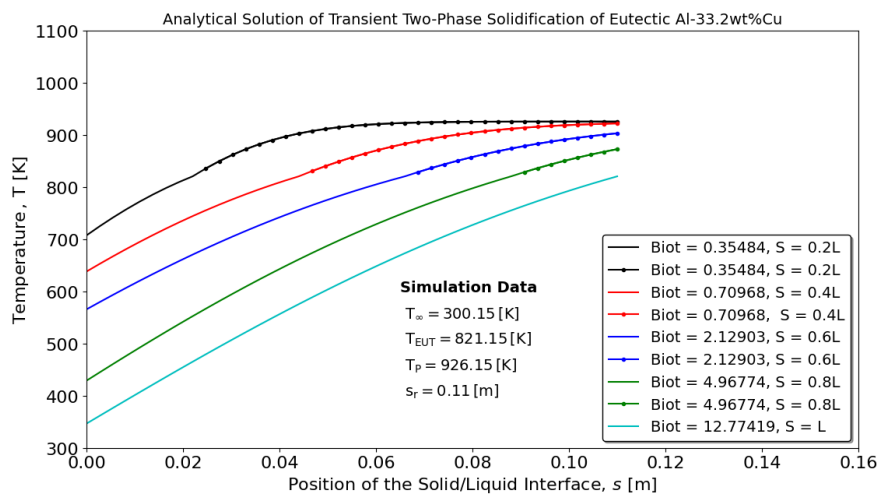




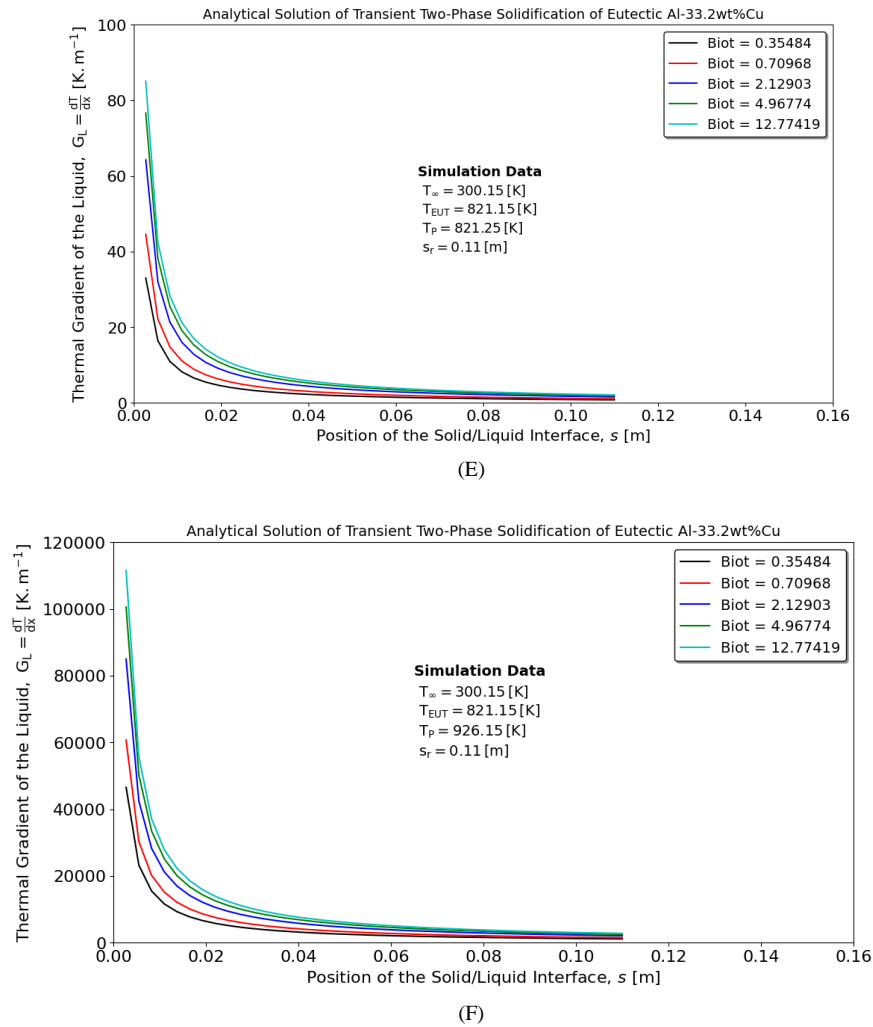
(B)



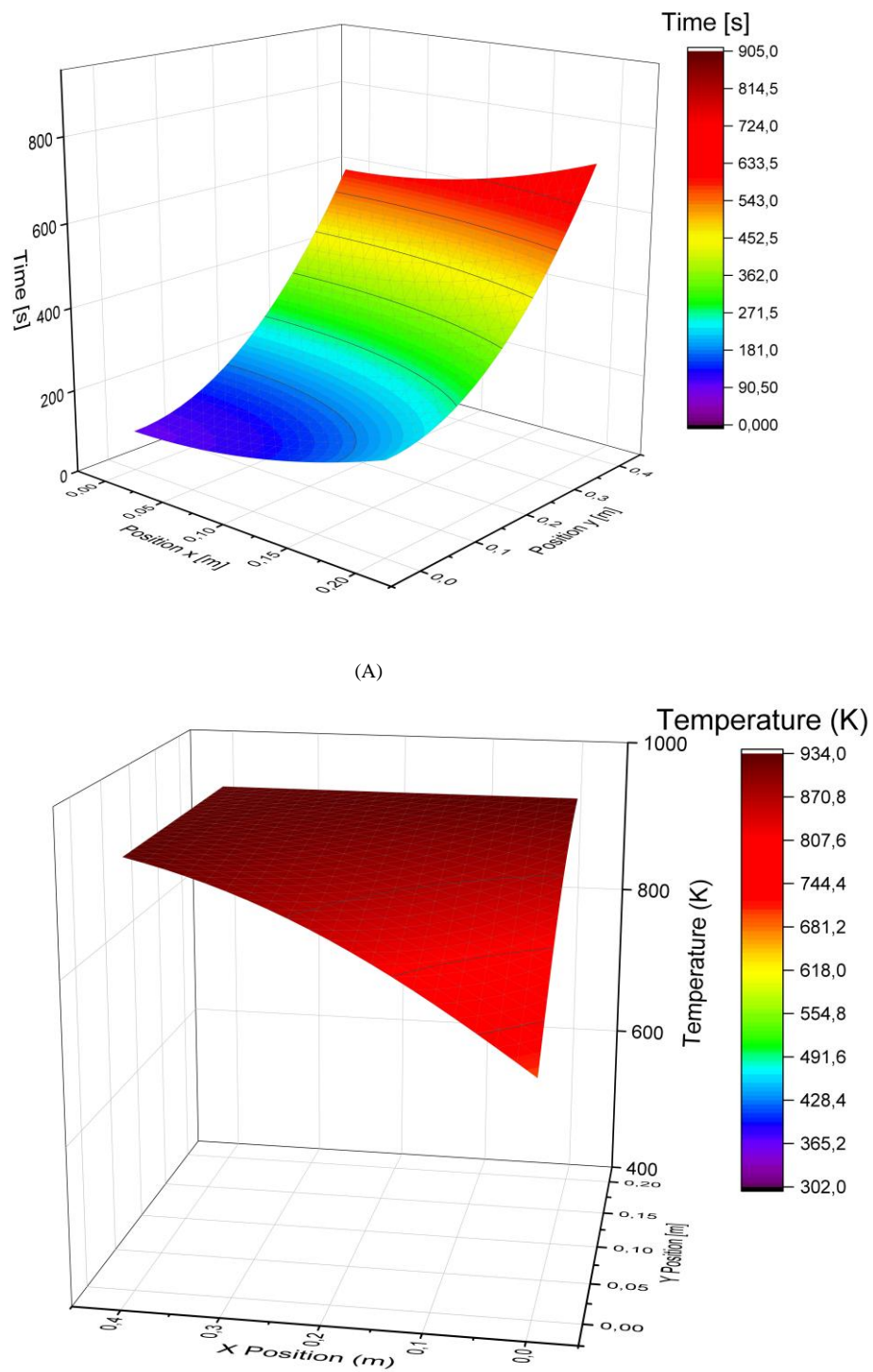
(C)



(D)



In the case of a three-dimensional solution for one-phase solidification, the time is presented as a function of $s = \sqrt{s_x^2 + s_y^2 + s_z^2}$ and the temperature profile $\frac{T_S(x,y,z,t) - T_F}{T_{\infty_i} - T_F}$, considering the following data: $h_x = 12000 \text{ W m}^{-2}\text{K}^{-1}$, $h_y = 7000 \text{ W m}^{-2}\text{K}^{-1}$ and $h_z = 300 \text{ W m}^{-2}\text{K}^{-1}$; $T_{\infty_x} = T_{\infty_y} = T_{\infty_z} = 303.15 \text{ K}$, $s_x = 0.2 \text{ m}$, $s_y = 0.4 \text{ m}$ and $s_z = 0.3 \text{ m}$. From Fig. 10, it can be noted that the parabolic profile is preserved, and shorter times are expected for the x and y directions. The lowest predicted temperature is associated with the direction of the highest heat transfer coefficient.



(A)

(B)

Figure 10 Analytical solution for three-dimensional one-phase solidification: (A) Position of solid/liquid interface as a function of time, and (B) Temperature profiles

Figures 11-13 present the solid-liquid interface velocity, the thermal gradient, and the cooling rate predicted by [64] alongside the current solution under 4% melt superheat for Al-33wt% Cu and Sn-39Pb eutectic alloys. Water behaves similarly in both eutectic alloys.

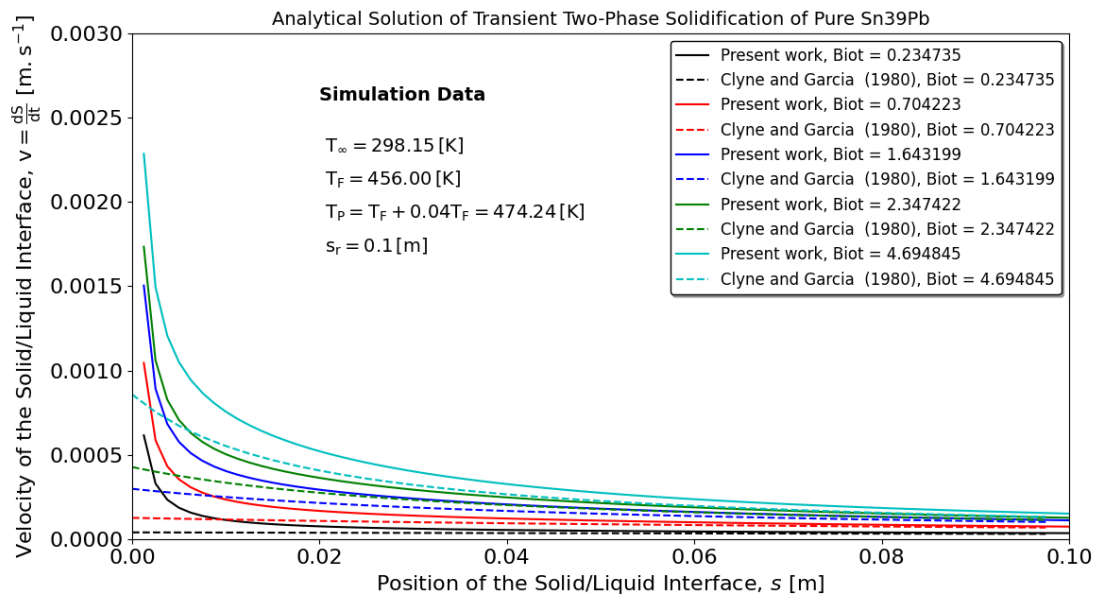
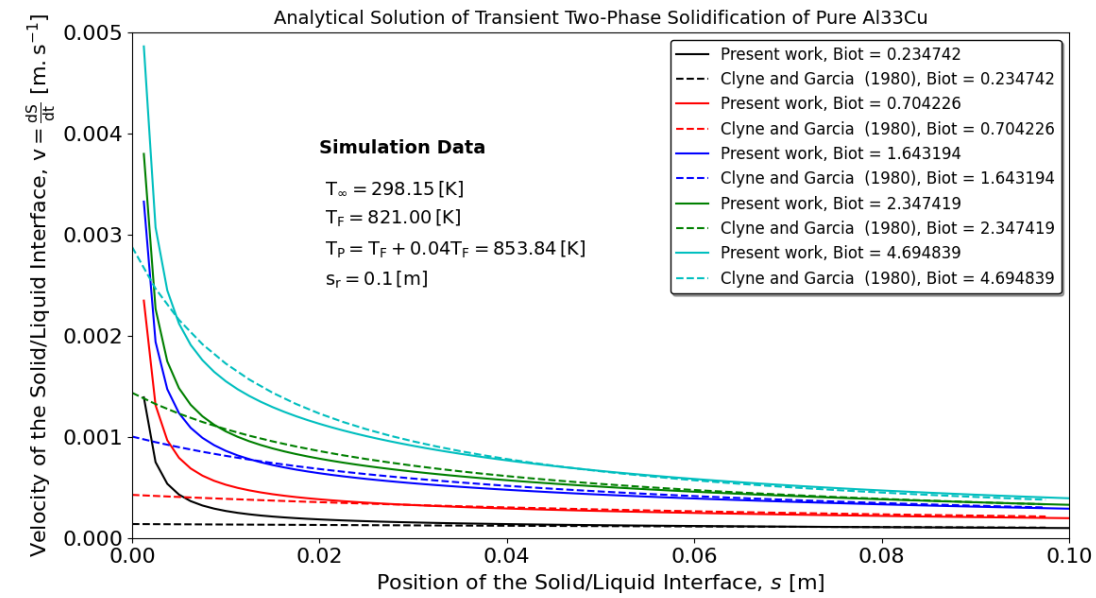


Figure 11 Comparison of analytical solutions for one-dimensional solidification solid-liquid interface velocities, considering eutectic alloys (A) Al33.2wt%Cu, and (B) Sn39wt%Pb under 4% superheat.

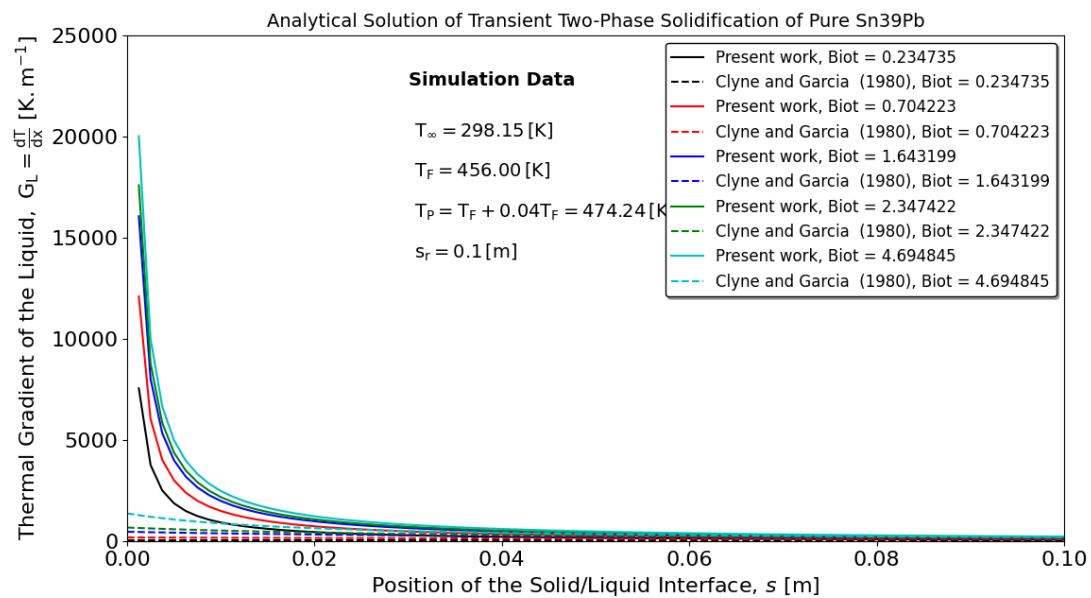
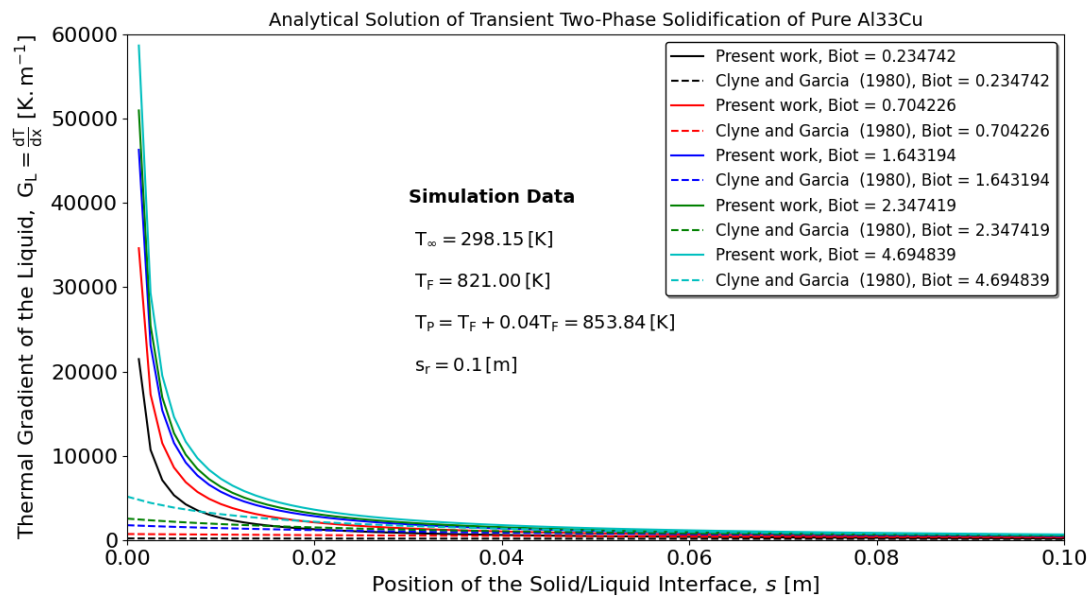


Figure 12 Comparison of analytical solutions for one-dimensional solidification thermal gradients, considering eutectic alloys (A) Al33.2wt%Cu, and (B) Sn39wt%Pb under 4% superheat.

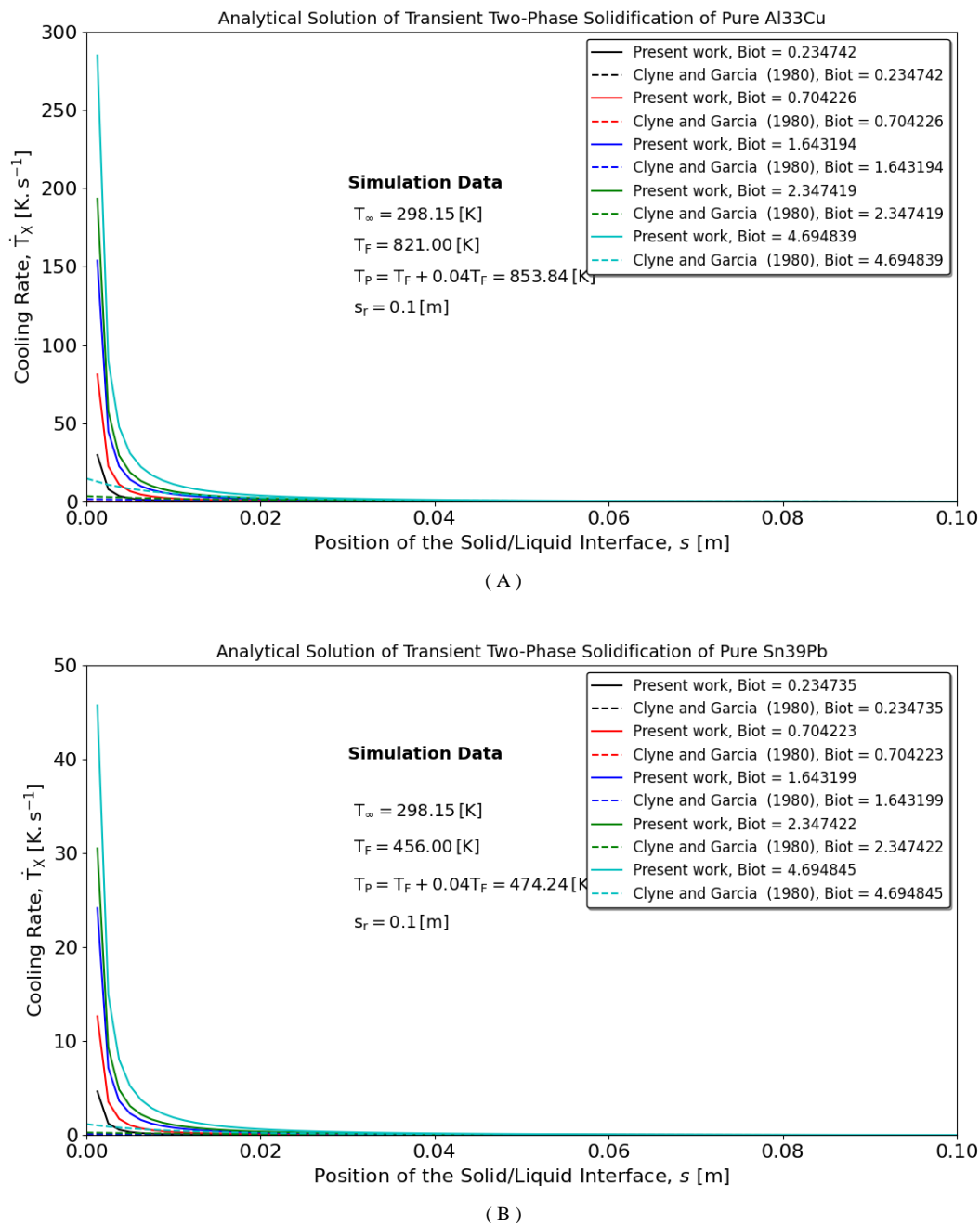
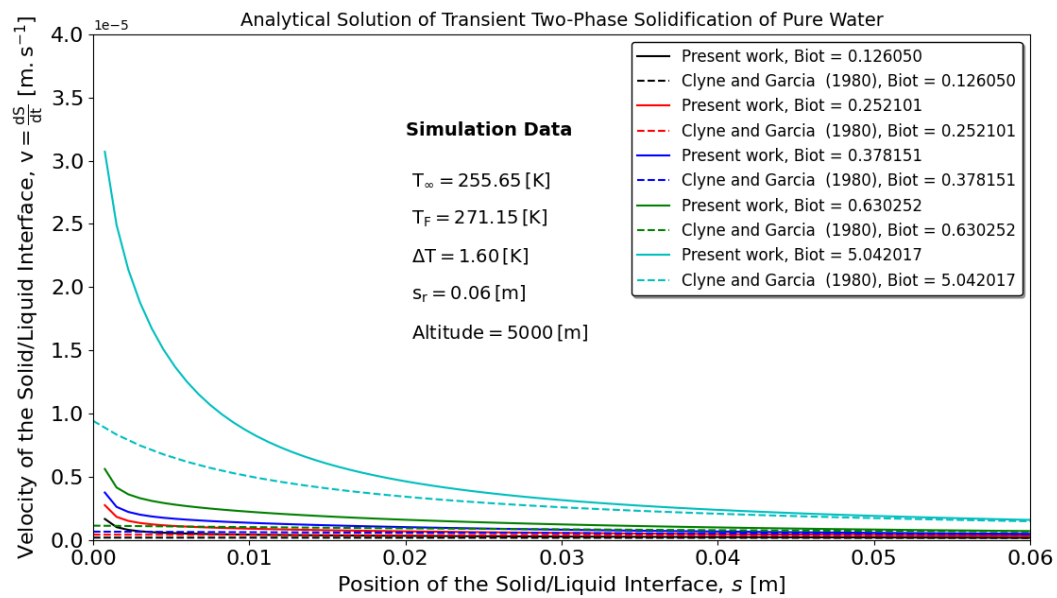
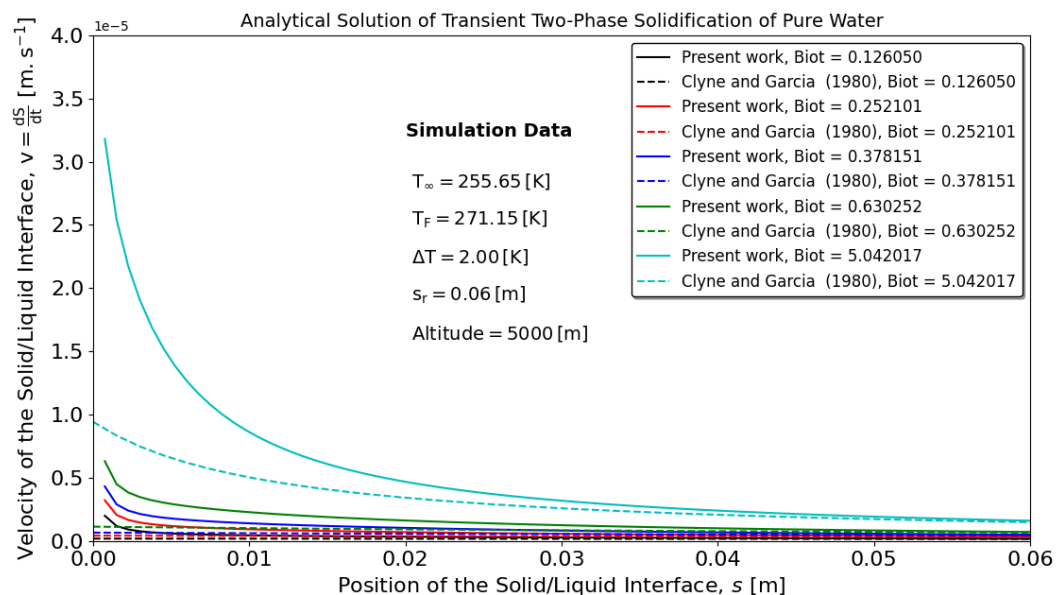


Figure 13 Comparison of analytical solutions for one-dimensional solidification cooling rates, considering eutectic alloys (A) Al33.2wt%Cu, and (B) Sn39wt%Pb under 4% superheat.

The final application of this analytical model is a comparison with a classical solidification model for pure and eutectic materials [64]. This analysis involves freezing water at an altitude of 5000 m to capture the surface thermal gradient. The present model can accommodate a wide range of Biot numbers, whereas [64] is limited to high Biot numbers, as shown in Figures14-16.

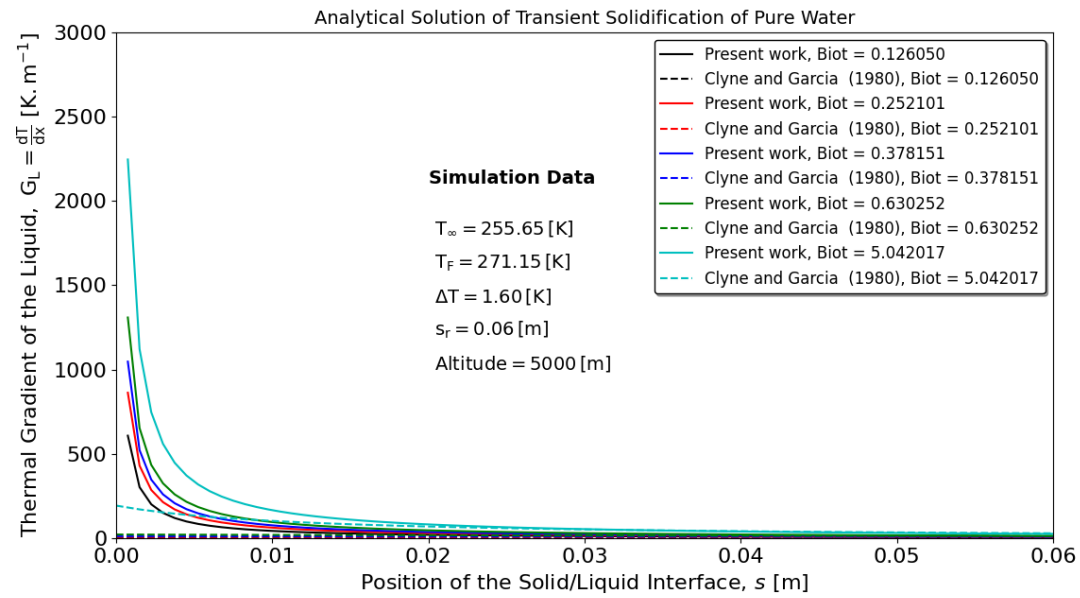


(A)

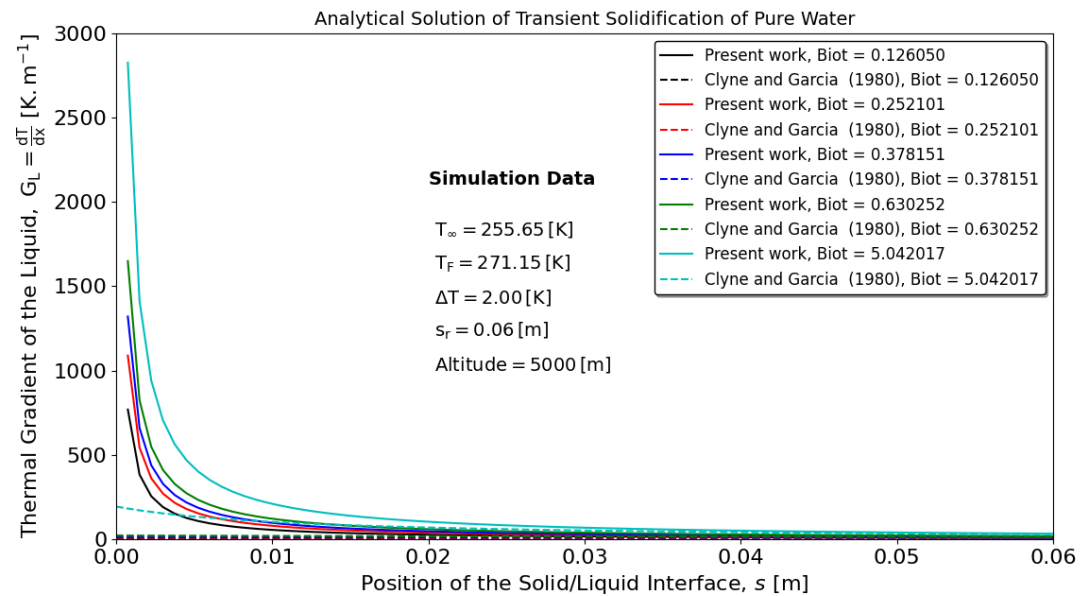


(B)

Figure 14 Comparison of analytical solutions for one-dimensional water freezing under solid-liquid interface velocities, considering (A) 1.6 K and (B) 2.0 K superheat.



(A)



(B)

Figure 15 Comparison of analytical solutions for one-dimensional water freezing under thermal gradients, considering (A) 1.6 K and (B) 2.0 K superheat.

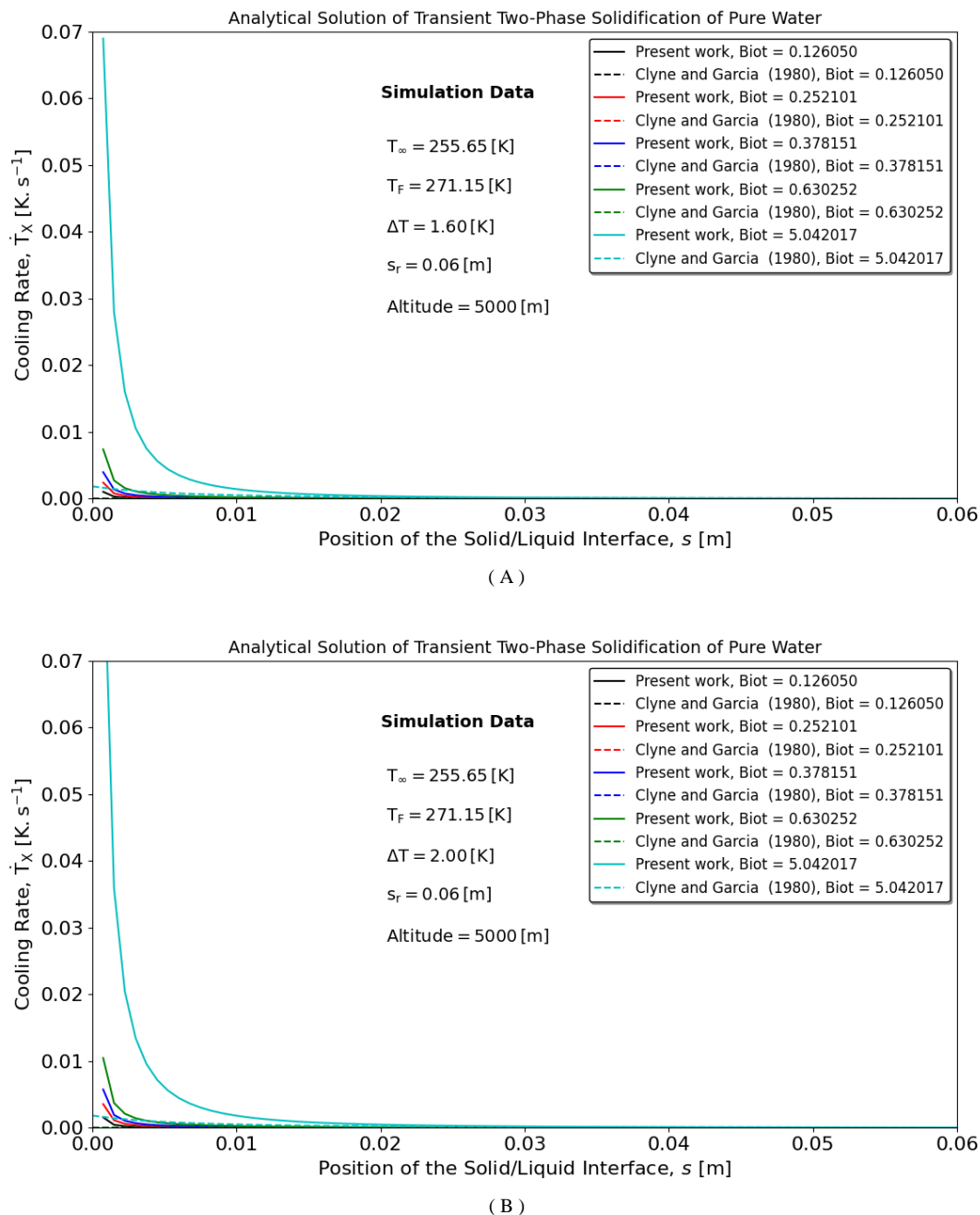


Figure 16 Comparison of analytical solutions for one-dimensional water freezing under cooling rate, considering (A) 1.6 K and (B) 2.0 K superheat.

IV. Conclusions

The following major conclusions can be drawn from the results and discussion held in this paper:

- Closed-form analytical solutions are derived for one- and two-phase, one- and three-dimensional transient solidification of pure and eutectic materials in a semi-infinite slab;
- The obtained analytical results and numerical values exhibited very good agreement;
- A closed-form solution for transient solidification considering convective boundary conditions that encompasses full analytical treatment of the Biot number has not yet been identified. Therefore, it was found that the proposed profile in the literature for the similarity variable based only on the assumption of the second-order parabolic term, i.e., $\frac{s^2}{4\alpha_S\phi^2}$, cannot deal with low Biot numbers in which a linear behaviour $\frac{k_S s}{2h\alpha_S}$ dominates;

- Considering the convective boundary conditions in the well-known analytical solution for heat conduction and using this approach to describe the one- and two-phase moving boundary interfaces, analytical solutions for transient solidification in a semi-infinite slab were obtained that can address anisotropic thermophysical properties;
- Investigations must be performed to elucidate the second-order polynomial dependence of the similarity variable in the proposition of transformation kinetics in addition to that tentatively suggested by Wagner, which has been widely used today in fluid flow, heat and mass transfer analytical solutions.

Declarations

Acknowledgements

The authors acknowledge the financial support provided by CAPES (Coordenação de Aperfeiçoamento de Pessoal de Nível Superior - Brazil), Finance Code 001, Grant 88881.707312/2022-01, and CNPq (National Council for Scientific and Technological Development - Brazil) Grant 301502/2022-6.

Author contributions

I.L. Ferreira developed the formalism, derived the equations proposed, and performed all the computations. GEM Santos Júnior wrote the introduction, review, references, and verified derivations. A.L.S. Moreira improved the text quality and revised the equations.

Conflicts of interest or competing interests

The authors declare that they have no known competing financial interests or personal relationships that could have appeared to influence the work reported in this paper.

Data and code availability

The data supporting this study's findings are available from the corresponding author upon reasonable request.

References

- [1] Rappaz, M. Modeling And Characterization Of Grain Structures Of Defects In Solidification. *Current Opinion In Solid State And Materials Science*, 2016; 20: 37-45.
- [2] Iten M, Liu S, Shukla A. A Review On The Air-PCM-TES Application For Free Cooling And Heating In The Buildings, *Renewable Sustainable Energy Rev* 2016; 61: 175-186.
- [3] Flemings, MC. *Solidification Processing*. New York: McGraw-Hill, 1974.
- [4] Wang D, Zhou C, Xu G, Huaiyuan A. Heat Transfer Behavior Of Top Side-Pouring Twin-Roll Casting. *Journal Of Materials Processing Technology*, 2014; 214: 1275-84.
- [5] Ozisik MN, *Finite Difference Methods In Heat Transfer*, 1st Edn. CRC Press, Boca Raton, 1994.
- [6] Carslaw HS, Jaeger JC. *Conduction Of Heat In Solids*. 2nd Ed. London: Oxford University Press; 1959.
- [7] Mori A, Akari K. Methods Of Analysis Of The Moving Boundary-Surface Problem. *Int. J. Chem. Eng.* 1976;16:734-744.
- [8] Alexandrov DV, Ivanov AA, Alexandrova IV. Analytical Solutions Of Mushy Layer Equations Describing Directional Solidification In The Presence Of Nucleation. *Philos Trans A Math Phys Eng Sci*. 2018; <https://doi.org/10.1098/Rsta.2017.0217>
- [9] Bouchard D, Kirkaldy JS. Prediction Of Dendrite Arm Spacings In Unsteady And Steady-State Heat Flow Of Unidirectionally Solidified Binary Alloys. *Metall Mater Trans B*. 1997;28:651-63.
- [10] Crank J. *Free And Moving Boundary Problems*. 2nd Ed. Oxford: Clarendon Press; 1984.
- [11] Crank J. How To Deal With Moving Boundaries In Thermal Problems. In: Lewis RW, Morgan K, Zienkiewicz OC, Editors. *Numerical Methods In Heat Transfer*. Chichester; New York: Wiley; 1981. Pp. 177-200.
- [12] Furzeland RM. A Survey Of The Formulation And Solution Of Free And Moving Boundary (Stefan) Problems. *Brunel University Mathematics Technical Papers Collection*. London; 1977.
- [13] Hunziker O. Theory Of Plane Front And Dendritic Growth In Multicomponent Alloys. *Acta Mater*. 2001;49:4191-203.
- [14] Rappaz M, Jacot A, Boettinger WJ. Last-Stage Solidification Of Alloys: Theoretical Model Of Dendrite-Arm And Grain Coalescence. *Metall Mater Trans A*. 2003;34:467-79.
- [15] Voller VR. Analytical Models Of Solidification Phenomena. *T Indian I Metals*. 2009;62:279-83.
- [16] Ferreira IL, Garcia A, Moreira ALS. On The Multiscale Formulation And The Derivation Of Phase- Change Moving Interfaces. *International Journal Of Thermophysics* 2023;44: 1-42 <https://doi.org/10.1007/S10765-022-03099-6>.
- [17] Ferreira IL, Moreira ALS. On The Continuous Mechanics First And Second-Order Formulations For Nonequilibrium Nucleation: Derivation And Applications. *Int J. Thermophys.* 2023;44:72 <https://doi.org/10.1007/S10765-023-03178-2>.
- [18] Chaurasiya V, Rai KN, Singh J. A Study Of Solidification On Binary Eutectic System With Moving Phase Change Material. *Therm. Sci. Eng. Prog.* 2021; 25:101002.
- [19] Chaurasiya V, Rai KN, Singh J. Heat Transfer Analysis For The Solidification Of A Binary Eutectic System Under Imposed Movement Of The Material. *J. Therm. Anal. Calorim.* 2022; 147:3229-46.
- [20] Ghanbar A, Ojo AO. Effect Of Nonplanar Geometry On Diffusion Kinetics During Brazing Repair Process. *Mater. Sci. Technol.* 2020;36:3.
- [21] Alkemper J, Voorhees PW. Three-Dimensional Characterization Of Dendritic Microstructures. *Acta Mater*. 2001;49:897-902.
- [22] Dousti P, Ranjbar AA, Famouri M, Ghaderi A. An Inverse Problem In Estimation Of Interfacial Heat Transfer Coefficient During Two-Dimensional Solidification Of Al5% Wt-Si Based On PSO. *Int J Num Meth Heat Fluid Flow*. 2010; 22:473-90.

- [23] Ferreira IL, Garcia A, Nestler B. On Macrosegregation In Ternary Al–Cu–Si Alloys: Numerical And Experimental Analysis. *Scripta Mater.* 2004;50:407-11.
- [24] Ferreira IL, Spinelli JE, Garcia A. Gravity-Driven Inverse Segregation During Transient Upward Directional Solidification Of Sn–Pb Hypoeutectic Alloys. *J Alloys Compd.* 2009; 475:396-400.
- [25] Gu C, Ridgeway CD, Luo AA. Examination Of Dendritic Growth During Solidification Of Ternary Alloys Via A Novel Quantitative 3D Cellular Automaton Model. *Metall Mater Trans B.* 2018; 50:123-35.
- [26] Jelinek B, Eshraghi M, Felicelli S, Peters JF. Large-Scale Parallel Lattice Boltzmann-Cellular Automaton Model Of Two-Dimensional Dendritic Growth. *Comput Phys Commun.* 2014; 185:939-47.
- [27] Li J, Wang Z, Wang Y, Wang J. Phase-Field Study Of Competitive Dendritic Growth Of Converging Grains During Directional Solidification. *Acta Mater.* 2012; 60:1478-93.
- [28] Swaminathan CR, Voller VR. Towards A General Numerical Scheme For Solidification Systems. *Int J Heat Mass Transfer.* 1997;40:2859-68.
- [29] Tan L, Zabaras N. Modeling The Growth And Interaction Of Multiple Dendrites In Solidification Using A Level Set Method. *J Comput Phys.* 2007;226:131-55.
- [30] Tang J, Xue X. Phase-Field Simulation Of Directional Solidification Of A Binary Alloy Under Different Boundary Heat Flux Conditions. *J Mater Sci.* 2009;44:745-53.
- [31] Trovant M, Argyropoulos SA. The Implementation Of A Mathematical Model To Characterize Mold-Metal Interface Effects In Metal Casting. *Can Metall Q.* 1998;37:185-96.
- [32] Zhang L, Li L. Determination Of Heat Transfer Coefficients At Metal/Chill Interface In The Casting Solidification Process. *Heat Mass Transfer.* 2013; 49:1071-80.
- [33] Zhu MF, Stefanescu DM. Virtual Front Tracking Model For The Quantitative Modeling Of Dendritic Growth In Solidification Of Alloys. *Acta Mater.* 2007;55:1741-55.
- [34] Acer E, Çadırli E, Erol H, Gündüz M. Effect Of Growth Rate On The Microstructure And Microhardness In A Directionally Solidified Al–Zn–Mg Alloy. *Metall Mater Trans A.* 2016;47:3040-51.
- [35] Acer E, Çadırli E, Erol H, Kaya H, Gündüz M. Effects Of Growth Rates And Compositions On Dendrite Arm Spacings In Directionally Solidified Al–Zn Alloys. *Metall Mater Trans A.* 2017;48:5911-23.
- [36] Barros A, Cruz C, Silva AP, Cheung N, Garcia A, Rocha O, Moreira A. Horizontally Solidified Al–3wt%Cu–(0.5wt%Mg) Alloys: Tailoring Thermal Parameters, Microstructure, Microhardness, And Corrosion Behavior. *Acta Metallurgica Sinica (English Letters).* 2019;32:695-709.
- [37] Bayram Ü, Maraşlı N. Thermal Conductivity And Electrical Resistivity Dependences On Growth Rate In The Directionally Solidified Al–Cu–Ni Eutectic Alloy. *J Alloys Compd.* 2018;753:695-702.
- [38] Carvalho D, Rodrigues J, Soares D, Aviz J, Barros A, Silva M, Rocha O, Ferreira I, Moreira A. Microindentation Hardness-Secondary Dendritic Spacings Correlation With Casting Thermal Parameters In An Al–9wt.%Si Alloy. *Mater Sci Medzg.* 2018;24:18-23.
- [39] Costa MO, Barbosa CR, Azevedo HM, Machado GH, Rocha FS, Moreira AS, Rocha OL. Thermal Analysis Via Horizontal Solidification Of Al₃Cu₂Si (Mass%) Alloy: Thermal And Microstructural Parameters, Intermetallic Compounds And Microhardness. *J Therm Anal Calorim.* 2021; <https://doi.org/10.1007/S10973-020-10419-1>
- [40] Dong X, Ji S. Si Poisoning And Promotion On The Microstructure And Mechanical Properties Of Al–Si–Mg Cast Alloys. *J Mater Sci.* 2018;53:7778-92.
- [41] Drevet B, Thi HN, Camel D, Billia B, Dupouy MD. Solidification Of Aluminium-Lithium Alloys Near The Cell/Dendrite Transition-Influence Of Solutal Convection. *J Cryst Growth.* 2000;218:419-33.
- [42] Ghoncheh MH, Shabestari SG, Abbasi MH. Effect Of Cooling Rate On The Microstructure And Solidification Characteristics Of Al₂O₃ Alloy Using Computer-Aided Thermal Analysis Technique. *J Therm Anal Calorim.* 2014;117:1253-61.
- [43] Hosseini VA, Shabestari SG, Gholizadeh R. Study On The Effect Of Cooling Rate On The Solidification Parameters, Microstructure, And Mechanical Properties Of LM13 Alloy Using Cooling Curve Thermal Analysis Technique. *Mater Des.* 2013;50:7-14.
- [44] Kaygısız Y, Maraşlı N. Microstructural, Mechanical, And Electrical Characterization Of Directionally Solidified Al–Cu–Mg Eutectic Alloy. *Phys Met Metallogr.* 2017;118:389-98.
- [45] Li M, Mori T, Iwasaki H. Effect Of Solute Convection On The Primary Arm Spacings Of Pb–Sn Binary Alloys During Upward Directional Solidification. *Mater Sci Eng A.* 1999;265:217-23.
- [46] Li X, Fautrelle Y, Ren Z. Influence Of Thermoelectric Effects On The Solid–Liquid Interface Shape And Cellular Morphology In The Mushy Zone During The Directional Solidification Of Al–Cu Alloys Under A Magnetic Field. *Acta Mater.* 2007;55:3803-13.
- [47] Li X, Gagnoud A, Fautrelle Y, Ren Z, Moreau R, Zhang Y, Esling C. Dendrite Fragmentation And Columnar-To-Equiaxed Transition During Directional Solidification At Lower Growth Speed Under A Strong Magnetic Field. *Acta Mater.* 2012;60:3321-32.
- [48] Li YZ, Mangelinck-Noël N, Zimmermann G, Sturz L, Nguyen-Thi H. Modification Of The Microstructure By Rotating Magnetic Field During The Solidification Of Al–7 Wt.% Si Alloy Under Microgravity. *J Alloys Compd.* 2020; <https://doi.org/10.1016/J.Jallcom.2020.155458>
- [49] Mckeown JT, Kulovits AK, Liu C, Zweigacker K, Reed BW, Lagrange T, Wiezorek JMK, Campbell GH. In Situ Transmission Electron Microscopy Of Crystal Growth-Mode Transitions During Rapid Solidification Of A Hypoeutectic Al–Cu Alloy. *Acta Mater.* 2014;65:56-68.
- [50] Ridgeway CD, Gu C, Luo AA. Predicting Primary Dendrite Arm Spacing In Al–Si–Mg Alloys: Effect Of Mg Alloying. *J Mater Sci.* 2019;54:9907-20.
- [51] Riestra M, Ghassemali E, Bogdanoff T, Seifeddine S. Interactive Effects Of Grain Refinement, Eutectic Modification And Solidification Rate On Tensile Properties Of Al–10Si Alloy. *Mater Sci Eng A.* 2017;703:270-9.
- [52] Şahin M, Şensoy T, Çadırli E. Microstructural Evolution And Mechanical Properties Of Sn–Bi–Cu Ternary Eutectic Alloy Produced By Directional Solidification. *Mater Res.* 2018; <https://doi.org/10.1590/1980-5373-MR-2017-0901>
- [53] Stan S, Chisamera M, Riposan I, Barstow M. Application Of Thermal Analysis To Monitor The Quality Of Hypoeutectic Cast Irons During Solidification In Sand And Metal Moulds. *J Therm Anal Calorim.* 2012;110:1185-92.
- [54] Beck JV. Nonlinear Estimation Applied To The Nonlinear Inverse Heat Conduction Problem. *Int. J. Heat Mass Transfer Vol.* 1970; 13:703-16
- [55] Loulou T, Artyukhin EA, Bardon JP. Estimation Of Thermal Contact Resistance During The First Stages Of Metal Solidification Process: I- Experiment Principle And Modelisation. *Int. J. Heat Mass Transfer.* 1999; 42: 2119-27

- [56] Piwonka T.S., Woodbury, K.A., Wiest JM. Modeling Casting Dimensions: Effect Of Wax Rheology And Interfacial Heat Transfer. Mater. Des. 2000;2:365-72
- [57] Ferreira IL, Spinelli JE, Pires JC, Garcia A. The Effect Of Melt Temperature Profile On The Transient Metal/Mold Heat Transfer Coefficient During Solidification. Mater. Sci. Eng. A. 2005;408:317-325
- [58] Trojan M. Transient Heat Conduction In Semi-Infinite Solid With Surface Convection. In: Hetnarski, R.B. (Eds) Encyclopedia Of Thermal Stresses. Springer, Dordrecht 2014 https://doi.org/10.1007/978-94-007-2739-7_415
- [59] Jost W. Diffusion In Solids, Liquids And Gases, Academic Press Inc.: New York. 1952.
- [60] Ferreira IL, C. A. Santos, Voller VR, Garcia A. Analytical, Numerical, And Experimental Analysis Of Inverse Segregation During Upward Unidirectional Solidification Of Al-Cu Alloys. Metall Mater Trans B. 2004;25: 285-97.
- [61] Ferreira IL, Voller VR, Nestler B, Garcia A. Two-Dimensional Numerical Model For The Analysis Of Macrosegregation During Solidification, Comp Mater Sci. 2009;46:358-66.
- [62] Garcia A., Prates M. Mathematical Model For The Unidirectional Solidification Of Metals: I. Cooled Molds, Metall. Trans. B. 1978; 9:449-457.
- [63] Garcia A., Clyne T.W., Prates M. Mathematical Model For The Unidirectional Solidification Of Metals: II. Massive Molds. Metall. Trans. B. 1979; 10:85-92
- [64] Clyne T.W., Garcia A. Assessment Of A New Model For Heat Flow During Unidirectional Solidification Of Metals. J. Heat Mass Transf. 1980; 23:773-782